Quantum Algorithms for Quantum Field Theories

Stephen P. Jordan,[1]* Keith S. M. Lee,[2] John Preskill[3]

Quantum field theory reconciles quantum mechanics and special relativity, and plays a central role in many areas of physics. We developed a quantum algorithm to compute relativistic scattering probabilities in a massive quantum field theory with quartic self-interactions (ϕ^4 theory) in spacetime of four and fewer dimensions. Its run time is polynomial in the number of particles, their energy, and the desired precision, and applies at both weak and strong coupling. In the strong-coupling and high-precision regimes, our quantum algorithm achieves exponential speedup over the fastest known classical algorithm.

The question whether quantum field theories can be efficiently simulated by quantum computers was first posed by Feynman three decades ago when he introduced the notion of quantum computers (*1*). Since then, efficient quantum algorithms for simulating the dynamics of quantum many-body systems have been developed theoretically (*2*–*4*) and demonstrated experimentally (*5*–*7*). Quantum field theory, which applies quantum mechanics to functions of space and time, presents additional technical challenges, because the number of degrees of freedom per unit volume is formally infinite.

We show that quantum computers can efficiently calculate scattering probabilities in continuum ϕ^4 theory to an arbitrary degree of precision. We have chosen ϕ^4 theory, a scalar theory with quartic self-interactions, because it is among the simplest interacting quantum field theories and thus illustrates essential issues without unnecessary complications. Our work introduces several new techniques, including creation of the initial state by a generalization of adiabatic state preparation and the use of effective field theory to analyze spatial discretization errors.

In complexity theory, the efficiency of an algorithm is judged by how its computational demands scale with the problem size or some other quantity associated with the problem's intrinsic difficulty. An algorithm with polynomial-time asymptotic scaling is considered to be feasible, whereas one with superpolynomial (typically, exponential) scaling is considered infeasible. This classification has proved to be a useful guide in practice.

Traditional calculations of quantum field theory scattering amplitudes rely on perturbation theory—namely, a series expansion in powers of the coupling (the coefficient of the interaction term), which is taken to be small. A powerful and intuitive way of organizing this perturbative expansion is through Feynman diagrams, in which the number of loops is associated with the power of the coupling. A reasonable measure of the computational complexity of perturbative calculations is therefore the number of Feynman diagrams, which is determined by combinatorics and grows factorially with the number of loops and the number of external particles.

If the coupling constant is insufficiently small, the perturbation series does not yield correct results. In ϕ^4 theory, for $D = 2$, 3 spacetime dimensions, by increasing the coupling λ_0, one eventually reaches a quantum phase transition at some critical coupling λ_c (*8*–*10*). In the parameter space near this phase transition, perturbative methods become unreliable; this region is referred to as the strong-coupling regime. There are then no known feasible classical methods for calculating scattering amplitudes, although lattice field theory can be used to obtain static quantities such as mass ratios. Even at weak coupling, the perturbation series is not convergent, although it is asymptotic (*11*–*13*). Including higher-order contributions beyond a certain point makes the approximation worse. There is thus a maximum possible precision achievable perturbatively.

We simulate a process in which initially well-separated massive particles with well-defined momenta scatter off each other. The input to our algorithm is a list of the momenta of the incoming particles, and the output is a list of the momenta of the outgoing particles produced by the physical scattering process. At relativistic energies, the number of outgoing particles may differ from the number of incoming particles. In accordance with quantum mechanics, the incoming momenta do not uniquely determine the outgoing momenta, but rather a probability distribution over possible outcomes. Upon repeated runs, our quantum algorithm samples from this distribution. The asymptotic scaling of the algorithm is given in Eq. 9 and Table 1. The simulated scattering processes closely match experiments in particle accelerators, which are the standard tools to probe quantum field-theoretical effects.

The issue of gauge symmetries in quantum simulation of lattice field theories has been addressed in (*14*). There is an extensive literature on analog simulation of interacting quantum field theories using ultracold atoms (*15*–*26*), trapped ions (*27*, *28*), and Josephson-junction arrays (*29*). Much work has also been done on analog simulation of special-relativistic quantum mechanical effects such as zitterbewegung and the Klein paradox, as well as general-relativistic quantum effects such as Hawking radiation [for recent reviews, see (*30*, *31*)]. Our work, in contrast to these studies, addresses digital quantum simulation, with explicit consideration of convergence to the continuum limit and efficient preparation of wave packet states for the computation of dynamical quantities such as scattering probabilities. Our analysis includes error estimates of all parts of our algorithm.

Representing fields with qubits. Although quantum field theory is typically expressed in terms of Lagrangians and within the interaction picture, our algorithm is more naturally described in the formalism of Hamiltonians and within the Schrödinger picture. We start by defining a lattice ϕ^4 theory and subsequently address convergence to the continuum theory. (In $D = 4$, the continuum limit is believed to be the free theory. Nonetheless, because the coupling shrinks only logarithmically, scattering processes for particles with small momenta in lattice units are interesting to compute.) Let $\Omega = a\mathbb{Z}_{\hat{L}}^d$, that is, an $\hat{L} \times ... \times \hat{L}$ lattice in $d = D - 1$ spatial dimensions with periodic boundary conditions and lattice spacing a. The number of lattice sites is $\mathcal{V} = \hat{L}^d$. For each $\mathbf{x} \in \Omega$, let $\phi(\mathbf{x})$ be a continuous, real degree of freedom—interpreted as the field at $\mathbf{x}$—and let $\pi(\mathbf{x})$ be the corresponding canonically conjugate variable. In canonical quantization, these degrees of freedom are promoted to Hermitian operators with the commutation relation

$$[\phi(\mathbf{x}), \pi(\mathbf{y})] = ia^{-d}\delta_{\mathbf{x},\mathbf{y}}\mathbb{1} \qquad (1)$$

We use units with $\hbar = c = 1$. ϕ^4 theory on the lattice Ω is defined by the Hamiltonian

$$H = \sum_{\mathbf{x}\in\Omega} a^d \left[\frac{1}{2}\pi(\mathbf{x})^2 + \frac{1}{2}(\nabla_a\phi)^2(\mathbf{x}) + \frac{1}{2}m_0^2\phi(\mathbf{x})^2 + \frac{\lambda_0}{4!}\phi(\mathbf{x})^4\right] \qquad (2)$$

where $\nabla_a\phi$ denotes a discretized derivative (that is, a finite-difference operator) and m_0 is the particle mass of the corresponding noninteracting ($\lambda_0 = 0$) theory.

[1]Applied and Computational Mathematics Division, National Institute of Standards and Technology, Gaithersburg, MD 20899, USA. [2]Pittsburgh Particle Physics, Astrophysics, and Cosmology Center, Department of Physics and Astronomy, University of Pittsburgh, Pittsburgh, PA 15260, USA. [3]Institute for Quantum Information and Matter, California Institute of Technology, Pasadena, CA 91125, USA.

*To whom correspondence should be addressed. E-mail: stephen.jordan@nist.gov

We represent the state of the lattice field theory by devoting one register of qubits to store the value of the field at each lattice point. In principle, each $\phi(\mathbf{x})$ is an unbounded continuous variable. To represent the field at a given site with finitely many qubits, we cut off the field at a maximum magnitude ϕ_{max} and discretize it in increments of δ_ϕ. This requires $n_b = O(\log_2(\phi_{max}/\delta_\phi))$ qubits per site. Note that this field discretization is a separate issue from the spatial discretization via the lattice Ω.

Let $|\psi\rangle$ be any state such that $\langle\psi|H|\psi\rangle \leq E$. The probability distribution over $\phi(\mathbf{x})$ defined by $|\psi\rangle$ (for any $\mathbf{x} \in \Omega$) yields a very low probability (*32*, *33*) for $|\phi(\mathbf{x})|$ to be much larger than $O(E^{1/2})$. Thus, a cutoff $\phi_{max} = O((\mathcal{V}E/a^d m_0^2\varepsilon)^{1/2})$ suffices to ensure fidelity $1 - \varepsilon$ to the original state $|\psi\rangle$. One can prove this by bounding $\langle\psi|\phi(\mathbf{x})|\psi\rangle$ and $\langle\psi|\phi^2(\mathbf{x})|\psi\rangle$ as functions of E and applying Chebyshev's inequality (*33*). To choose δ_ϕ, note that the eigenbasis of $a^d\pi(\mathbf{x})$ is the Fourier transform of the eigenbasis of $\phi(\mathbf{x})$. Hence, discretizing $\phi(\mathbf{x})$ in units of δ_ϕ is equivalent to introducing the cutoff $-\pi_{max} \leq \pi(\mathbf{x}) \leq \pi_{max}$, where $\pi_{max} = 1/(a^d\delta_\phi)$. By bounding the expectations of $\pi(\mathbf{x})$ and $\pi^2(\mathbf{x})$, one finds that it suffices to choose $\pi_{max} = O((\mathcal{V}E/\varepsilon a^d)^{1/2})$, and thus $n_b = O(\log_2(\mathcal{V}E/m_0\varepsilon))$.

The algorithm. We now turn to the main three tasks of quantum simulation: preparing an initial state, simulating the time evolution, and measuring final observables. We first discuss the simulation of time evolution because it is used in all three tasks. The unitary operator representing time evolution, $\exp(-iHt)$, can be approximated by a quantum circuit of $O((t\mathcal{V})^{1+(1/2k)})$ gates implementing a kth-order Suzuki-Trotter formula (*34*, *35*). For n time steps, the error is $\varepsilon \sim n^{-2k}$. The near-linear scaling with t has long been known. The scaling with $\mathcal{V}$ is a consequence of the locality of H (*33*) and appears not to have been noted previously in the quantum algorithms literature.

To simulate scattering, one needs to prepare an initial state of particles in well-separated wave packets. We do so by preparing the vacuum of the $\lambda_0 = 0$ theory, exciting wave packets, and then adiabatically turning on the coupling λ_0. Let $H^{(0)}$ be the Hamiltonian obtained by setting $\lambda_0 = 0$ in H. $H^{(0)}$ defines an exactly solvable model in which the particles are noninteracting. The vacuum (ground) state $|\mathrm{vac}(0)\rangle$ of $H^{(0)}$ is a multivariate Gaussian wave function in the variables $\{\phi(\mathbf{x})|\mathbf{x} \in \Omega\}$ and can therefore be prepared via the method of Kitaev and Webb (*36*). The asymptotic scaling of the Kitaev-Webb method is dictated by the computation of the $\mathbf{LDL}^T$ decomposition of the inverse covariance matrix, which can be done classically in $O(\mathcal{V}^{2.376})$ time (*37*, *38*).

In analogy with the harmonic oscillator, one can define creation and annihilation operators $a_\mathbf{p}$ and $a_\mathbf{p}^\dagger$ such that $H^{(0)} = \sum_{\mathbf{p}\in\Gamma} L^{-d}\omega(\mathbf{p})a_\mathbf{p}^\dagger a_\mathbf{p} + E^{(0)}\mathbb{1}$, where $\Gamma = (2\pi/\hat{L}a)\mathbb{Z}_{\hat{L}}^d$ is the momentum-space lattice corresponding to Ω, $\omega(\mathbf{p}) = [m_0^2 + (4/a^2)\sum_{j=1}^d \sin^2(ap_j/2)]^{1/2}$, and $E^{(0)}$ is an irrelevant zero-point energy. The operator $a_\mathbf{p}^\dagger$ can be interpreted as creating a (completely delocalized) particle of the noninteracting theory with momentum $\mathbf{p}$ and energy $\omega(\mathbf{p})$.

The (unnormalized) state $\phi(\mathbf{x})|\mathrm{vac}(0)\rangle$ is interpreted as a single particle localized at $\mathbf{x}$ [see, e.g., (*39*)]. Because $a_\mathbf{p}|\mathrm{vac}(0)\rangle = 0$, $\phi(\mathbf{x})|\mathrm{vac}(0)\rangle = a_\mathbf{x}^\dagger|\mathrm{vac}(0)\rangle$, where

$$a_\mathbf{x}^\dagger = \sum_{\mathbf{p}\in\Gamma} L^{-d}\exp(-i\mathbf{p}\cdot\mathbf{x})\left[\frac{1}{2\omega(\mathbf{p})}\right]^{1/2} a_\mathbf{p}^\dagger \quad (3)$$

The operator

$$a_\psi^\dagger = \eta(\psi)\sum_{\mathbf{x}\in\Omega} a^d\psi(\mathbf{x})a_\mathbf{x}^\dagger \quad (4)$$

creates a wave packet with position-space wave function ψ; $\eta(\psi)$ is a normalization constant, chosen so that $[a_\psi, a_\psi^\dagger] = 1$. $a_\psi^\dagger$ is not unitary, so it cannot be directly implemented by a quantum circuit. Instead, we introduce an ancillary qubit and let

$$H_\psi = a_\psi^\dagger\otimes|1\rangle\langle 0| + a_\psi\otimes|0\rangle\langle 1| \quad (5)$$

One can verify that $\exp(-iH_\psi\pi/2)|\mathrm{vac}(0)\rangle|0\rangle = -ia_\psi^\dagger|\mathrm{vac}(0)\rangle|1\rangle$. Using a high-order Suzuki-Trotter formula (*34*, *35*), we can construct an efficient quantum circuit approximating the unitary transformation $\exp(-iH_\psi\pi/2)$. Applied to $|\mathrm{vac}(0)\rangle$, this circuit yields the desired state up to an irrelevant global phase and an unentangled ancillary qubit, which can be discarded. We repeat this process for each incoming particle desired.

Because we wish to create localized wave packets, we choose $\psi(\mathbf{x})$ to have bounded support. Expanding $a_\psi^\dagger$ in terms of the operators ϕ and π yields an expression of the form $a_\psi^\dagger = \sum_{\mathbf{x}\in\Omega}[f(\mathbf{x})\phi(\mathbf{x}) + g(\mathbf{x})\pi(\mathbf{x})]$, where $f(\mathbf{x})$ and $g(\mathbf{x})$ are exponentially decaying with characteristic length scale $1/m_0$ outside the support of ψ. Thus, a_ψ and $a_\psi^\dagger$ can be exponentially well approximated by linear combinations of the operators ϕ and π on a local region of space, and the complexity of simulating $\exp(-iH_\psi\pi/2)$ does not scale with the volume V. Furthermore, provided the initial wave packets are separated by a distance δ that is large relative to $1/m_0$, the preparation of each additional wave packet leaves the existing wave packets almost perfectly undisturbed [with errors on the order of $\exp(-m_0\delta)$].

At this point, we have finished constructing wave packets of the noninteracting theory. We next use a Suzuki-Trotter formula to construct a quantum circuit simulating the unitary transformation induced by a time-dependent Hamiltonian in which the coupling constant is gradually increased from zero to its final value, λ_0, over time τ. A perfectly adiabatic turn-on would ensure that no stray particles are created during this process, provided particle creation costs energy, that is, the particles have nonzero mass. Imperfect adiabaticity causes errors, namely, particle creation from the vacuum and the splitting of one particle into three. The probabilities of such errors depend significantly on the particle mass.

In the $D = 2$, 3 interacting theory, with fixed m_0 and sufficiently large λ_0, the mass vanishes. This marks the location of the $\phi \to -\phi$ symmetry-breaking transition. Here, we restrict our attention to simulations within the symmetric phase, but we do consider systems arbitrarily close to the phase transition, because these should be particularly hard to simulate classically. In this regime, the mass exhibits known power-law behavior.

As Eq. 4 shows, wave packets are not eigenstates of $H^{(0)}$. During the adiabatic turn-on, the different eigenstates acquire different dynamical phases. Thus, as the wave packet time evolves, it propagates and broadens. This behavior is undesirable in our simulation, because we do not wish the particles to collide and scatter before the coupling reaches its final value. We therefore introduce backward time evolutions governed by time-independent Hamiltonians into the adiabatic state-preparation process to undo the dynamical phases. Specifically, let $H(s)$ parameterize the adiabatic time evolution, with $H(0) = H^{(0)}$ and $H(1) = H$. We divide the adiabatic preparation into J steps, with U_j denoting the unitary time evolution induced by the time-dependent Hamiltonian linearly interpolating between $H((j-1)/J)$ and $H(j/J)$ over a period of τ/J. Let M_j consist of backward, forward, and backward evolutions, namely,

$$M_j = \exp\left[iH\left(\frac{j+1}{J}\right)\frac{\tau}{2J}\right]U_j\exp\left[iH\left(\frac{j}{J}\right)\frac{\tau}{2J}\right] \quad (6)$$

Our full state-preparation process is $\prod_{j=1}^J M_j$. The dynamical phases are undone, converging to zero as $J \to \infty$, while the adiabatic change of eigenbasis is undisturbed (*33*).

What is the complexity of adiabatic state preparation? At weak coupling for $d = 1$, 2, a wave packet travels a distance $O(\tau/J^2)$ as the coupling is turned on; therefore, choosing $J = O(\tau^{1/2})$ ensures that this distance is a suitably small constant. Diabatic transitions occur with probability $O((J/\tau\gamma^2)^2)$, where γ is the energy gap of the transition; hence, the state preparation error is $\varepsilon = O(1/\tau)$. The number of quantum gates needed to simulate this process is $O((\tau\mathcal{V})^{1+o(1)}) = O((\tau a^{-d})^{1+o(1)})$ in a fixed physical volume; setting $\tau = O(\varepsilon^{-1})$ and $a = O(\varepsilon^{1/2})$ (see below), we conclude that the complexity scales as $O((1/\varepsilon)^{1+(d/2)})$. For $d = 3$, the scaling with ε is further enhanced because the perturbative corrections to the physical mass are highly sensitive to the value of a. Complexity scalings at strong coupling can be obtained by analogous reasoning (*33*).

After the system has evolved for a period in which scattering occurs, measurement can be performed in one of two ways. The interaction can be adiabatically turned off through the time-reversed version of the turn-on described above; in the free theory, we can then measure the number operators of the momentum modes, using the

method of phase estimation (*40*), that is, by simulating $\exp(iL^{-d}a_{\mathbf{p}}^{\dagger}a_{\mathbf{p}}t)$ for various values of t and Fourier-transforming the results. Alternatively, one can divide space into small regions and measure the total energy and momentum operators in each region using phase estimation. This is a reasonable idealization of real detectors and can yield information about bound-state energies.

Discretization errors. Having described how to simulate scattering processes in a discretized quantum field theory, we now consider discretization errors. To analyze these errors, we use methods of effective field theory (EFT), a well-developed formalism underlying our modern understanding of quantum field theory.

In its regime of validity, typically below a particular energy scale, an EFT reproduces the behavior of the full (that is, fundamental) theory under consideration: It can be regarded as the low-energy limit of that theory. An EFT for a full theory is thus somewhat analogous to a Taylor series for a function. It involves an expansion in some suitable small parameter, so that, although it consists of infinitely many terms, higher-order terms are increasingly suppressed. Thus, the series can be truncated, with corresponding finite and controllable errors.

We apply this framework to analyze the effect of discretizing the spatial dimensions of the continuum ϕ^4 quantum field theory. The discretized Lagrangian can be thought of as the leading contribution (denoted by $\mathcal{L}^{(0)}$) to an EFT. From the leading operators left out, we can thus infer the scaling of the error associated with a nonzero lattice spacing a.

The full (untruncated) effective Lagrangian will have every coupling respecting the $\phi \to -\phi$ symmetry and so will take the form

$$\mathcal{L}_{\text{eff}} = \mathcal{L}^{(0)} + \frac{c}{6!}\phi^6 + c'\phi^3\partial^2\phi + \frac{c''}{8!}\phi^8 + \cdots \tag{7}$$

This can be simplified. First, the chain rule and integration by parts can be used to write any operator with two derivatives acting on different fields in the form $\phi^n\partial^2\phi$. For example, $\phi^2\partial_\mu\phi\partial^\mu\phi = (1/3)\partial_\mu(\phi^3)\partial^\mu\phi \to -(1/3)\phi^3\partial^2\phi$. Such an operator can then be simplified via the equation of motion (*41*, *42*). If this were the equation of motion of the continuum theory, any derivative operator would then be completely eliminated. In the discretized theory, however, the equation of motion is modified and there are residual, Lorentz-violating operators. In fact, because the difference operators in the discretized theory are only approximately equal to the derivatives in the continuum theory, the simplest Lorentz-violating operators are induced purely by discretization.

In units where $\hbar = c = 1$, all quantities have units of some power of mass. The mass dimensions (denoted by square brackets) of the field and coupling in $D = d + 1$ spacetime dimensions are $[\phi] = (D-2)/2$ and $[\lambda] = 4 - D$, implying that

$$[c] = 6 - 2D, [c''] = 8 - 3D \tag{8}$$

In $D = 4$ dimensions, $[c] = -2$ and $[c''] = -4$, and the only pertinent dimensionful parameter is the lattice spacing; therefore, $c \sim a^2$ and $c'' \sim a^4$. Thus, of the operators not included in the Lagrangian $\mathcal{L}^{(0)}$, ϕ^6 is more significant than ϕ^{2n}, for $n > 3$.

In $D = 2, 3$, the scaling of the coefficients with a is somewhat less obvious, because now the coupling λ provides another dimensionful parameter. To obtain the scaling of c, one should consider the Feynman diagram that generates the corresponding operator. This involves three ϕ^4 vertices, so

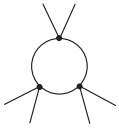

$$\sim \lambda^3 a^{6-D}$$

(Other diagrams involve higher powers of λ; hence their contributions to the operator are suppressed by higher powers of a.) Likewise, the coefficient of ϕ^8 will scale as $\lambda^4 a^{8-D}$, which means that it is suppressed by a^2 relative to the coefficient of ϕ^6.

The EFT thus consists of three different classes of operators: operators of the form ϕ^{2n}, Lorentz-violating operators arising solely from discretization effects, and Lorentz-violating operators resulting from discretization and quantum effects. These are shown with the scaling of their coefficients in Table 2, which reveals that the dominant discretization errors scale as a^2 in $D = 2, 3, 4$. (In $D = 2, 3$, errors of type II dominate. In $D = 4$, errors of types I and II each scale as a^2.)

At strong coupling, the operators and their scaling remain the same at the scale of the matching of the full theory onto the EFT, although the explicit coefficients are no longer calculable. However, the running of the coefficients down to lower energies is determined by their so-called anomalous dimensions, which depend on the coupling strength. These anomalous dimensions modify the scaling; at weak coupling the modification is small, but at strong coupling it could be larger. (Still, the scaling will remain polynomial.)

Concluding remarks. The most computationally costly part of the algorithm is either adiabatic state preparation or preparation of the free vacuum, depending on the asymptotic scaling considered and the number of spatial dimensions (*33*). Because $a \sim \varepsilon^{1/2}$, preparation of the free vacuum has complexity $\sim \mathcal{V}^{2.376} \sim a^{-2.376d} \sim \varepsilon^{2.376d/2}$. The number of gates, G_{weak}, needed to simulate weakly coupled, $(d+1)$-dimensional ϕ^4 theory with accuracy $\pm\varepsilon$ scales as follows:

$$G_{\text{weak}} \sim \begin{cases} \left(\frac{1}{\varepsilon}\right)^{1.5+o(1)}, & d = 1 \\ \left(\frac{1}{\varepsilon}\right)^{2.376+o(1)}, & d = 2 \\ \left(\frac{1}{\varepsilon}\right)^{5.5+o(1)}, & d = 3 \end{cases} \tag{9}$$

The notation $f(n) = o(g(n))$ means $\lim_{n\to\infty} f(n)/g(n) = 0$. The asymptotic scaling of the number of gates used to simulate the strongly coupled theory is summarized in Table 1. The minimum number of (perfect) qubits required for a nontrivial simulation in $D = 2$ is estimated—necessarily crudely—to be on the order of 1000 to 10,000, corresponding to ε ranging from 10% to 1% (*33*).

We have shown that quantum computers can efficiently calculate scattering probabilities in ϕ^4 theory to arbitrary precision at both weak and strong coupling. Known classical algorithms take exponential time to do this in the strong-coupling and high-precision regimes. In addition to establishing a new exponential quantum speedup, our results lead the way toward a quantum algorithm for simulating the Standard Model of particle physics, which has new features (not exhibited by ϕ^4 theory) such as chiral fermions and gauge interactions. Such an algorithm would establish that, except for quantum-gravity effects, the standard quantum circuit model suffices to capture completely the computational power of our universe.

Table 1. The asymptotic scaling of the number of quantum gates needed to simulate scattering in the strong-coupling regime in $d = 1, 2$ spatial dimensions is polynomial in p (the momentum of the incoming pair of particles), $\lambda_c - \lambda_0$ (the distance from the phase transition), and n_{out} (the maximum kinematically allowed number of outgoing particles). The notation $f(n) = \tilde{O}(g(n))$ means $f(n) = O(g(n)\log^c(n))$ for some constant c.

	$\lambda_c - \lambda_0$	p	n_{out}
$d = 1$	$\left(\frac{1}{\lambda_c - \lambda_0}\right)^{9+o(1)}$	$p^{4+o(1)}$	$\tilde{O}(n_{\text{out}}^5)$
$d = 2$	$\left(\frac{1}{\lambda_c - \lambda_0}\right)^{6.3+o(1)}$	$p^{6+o(1)}$	$\tilde{O}(n_{\text{out}}^{7.128})$

Table 2. Effective field theory operators fall into three classes. The general operator in each class is shown, with the canonical scaling of its coefficient in D spacetime dimensions. $\partial_x^{2l} = \sum_{i=1}^{d}\partial_i^{2l}$.

Class	Operators	Scaling of coupling
I	ϕ^{2n} $(n \geq 3)$	$\lambda^n a^{2n-D}$
II	$\phi\partial_x^{2l}\phi$ $(l \geq 2)$	a^{2l-2}
III	$\phi^{2j+1}\partial_x^{2l}\phi$ $(j \geq 1, l \geq 2)$	$\lambda^{j+1}a^{2j+2l+2-D}$

References and Notes

1. R. P. Feynman, *Int. J. Theor. Phys.* **21**, 467 (1982).
2. S. Lloyd, *Science* **273**, 1073 (1996).
3. D. S. Abrams, S. Lloyd, *Phys. Rev. Lett.* **79**, 2586 (1997).
4. C. Zalka, *Proc. R. Soc. London Ser. A* **454**, 313 (1998).
5. B. P. Lanyon *et al.*, *Science* **334**, 57 (2011).
6. M. Müller, K. Hammerer, Y. L. Zhou, C. F. Roos, P. Zoller, *New J. Phys.* **13**, 085007 (2011).
7. J. T. Barreiro *et al.*, *Nature* **470**, 486 (2011).
8. J. Glimm, A. Jaffe, *Phys. Rev. D* **10**, 536 (1974).
9. F. Guerra, L. Rosen, B. Simon, *Commun. Math. Phys.* **41**, 19 (1975).
10. O. A. McBryan, J. Rosen, *Commun. Math. Phys.* **51**, 97 (1976).
11. K. Osterwalder, R. Sénéor, *Helv. Phys. Acta* **49**, 525 (1976).
12. J.-P. Eckmann, H. Epstein, J. Fröhlich, *Ann. Inst. Henri Poincaré A* **25**, 1 (1976).
13. F. Constantinescu, *Ann. Phys.* **108**, 37 (1977).
14. T. Byrnes, Y. Yamamoto, *Phys. Rev. A* **73**, 022328 (2006).
15. H. P. Büchler, M. Hermele, S. D. Huber, M. P. A. Fisher, P. Zoller, *Phys. Rev. Lett.* **95**, 040402 (2005).
16. E. Zohar, B. Reznik, *Phys. Rev. Lett.* **107**, 275301 (2011).
17. G. Szirmai, E. Szirmai, A. Zamora, M. Lewenstein, *Phys. Rev. A* **84**, 011611(R) (2011).
18. J. I. Cirac, P. Maraner, J. K. Pachos, *Phys. Rev. Lett.* **105**, 190403 (2010).
19. L. Mazza *et al.*, *New J. Phys.* **14**, 015007 (2012).
20. E. Kapit, E. Mueller, *Phys. Rev. A* **83**, 033625 (2011).
21. A. Bermudez *et al.*, *Phys. Rev. Lett.* **105**, 190404 (2010).
22. P. Maraner, J. K. Pachos, *Phys. Lett. A* **373**, 2542 (2009).
23. L. Lepori, G. Mussardo, A. Trombettoni, *Europhys. Lett.* **92**, 50003 (2010).
24. K. Maeda, G. Baym, T. Hatsuda, *Phys. Rev. Lett.* **103**, 085301 (2009).
25. Á. Rapp, G. Zaránd, C. Honerkamp, W. Hofstetter, *Phys. Rev. Lett.* **98**, 160405 (2007).
26. H. Weimer, M. Müller, I. Lesanovsky, P. Zoller, H. P. Büchler, *Nat. Phys.* **6**, 382 (2010).
27. J. Casanova *et al.*, *Phys. Rev. Lett.* **107**, 260501 (2011).
28. J. Casanova, A. Mezzacapo, L. Lamata, E. Solano, http://arxiv.org/abs/1110.3730 (2011).
29. B. Douçot, L. B. Ioffe, J. Vidal, *Phys. Rev. B* **69**, 214501 (2004).
30. M. Lewenstein *et al.*, *Adv. Phys.* **56**, 243 (2007).
31. M. Johanning, A. Varón, C. Wunderlich, *J. Phys. B* **42**, 154009 (2009).
32. For $\lambda_0 > 0$ one has a tighter bound. In this case it is unlikely for $|\phi(\mathbf{x})|$ to be much larger than $O(E^{1/4})$.
33. See supplementary materials on *Science* Online.
34. M. Suzuki, *Phys. Lett. A* **146**, 319 (1990).
35. D. Berry, G. Ahokas, R. Cleve, B. C. Sanders, *Commun. Math. Phys.* **270**, 359 (2007).
36. A. Kitaev, W. A. Webb, http://arxiv.org/abs/0801.0342 (2008).
37. J. R. Bunch, J. E. Hopcroft, *Math. Comput.* **28**, 231 (1974).
38. D. Coppersmith, S. Winograd, *J. Symbolic Comp.* **9**, 251 (1990).
39. M. E. Peskin, D. V. Schroeder, *An Introduction to Quantum Field Theory* (Westview, Boulder, CO, 1995).
40. A. Y. Kitaev, http://arxiv.org/abs/quant-ph/9511026 (1995).
41. C. Arzt, *Phys. Lett. B* **342**, 189 (1995).
42. H. Georgi, *Nucl. Phys. B* **361**, 339 (1991).

Acknowledgments: We thank A. Gorshkov for helpful discussions. Supported by NSF grant PHY-0803371, U.S. Department of Energy grant DE-FG03-92-ER40701, and NSA/Army Research Office grant W911NF-09-1-0442. Much of this work was done while S.P.J. was at the Institute for Quantum Information (IQI), Caltech, supported by the Sherman Fairchild Foundation. K.S.M.L. was supported in part by NSF grant PHY-0854782. He is grateful for the hospitality of the IQI, Caltech, during parts of this work.

Supplementary Materials

www.sciencemag.org/cgi/content/full/336/6085/1130/DC1
Texts S1 to S7
Figs. S1 and S2
References (*43*–*47*)

24 November 2011; accepted 5 April 2012
10.1126/science.1217069

The Detection and Characterization of a Nontransiting Planet by Transit Timing Variations

David Nesvorný,[1]* David M. Kipping,[2] Lars A. Buchhave,[3,4] Gáspár Á. Bakos,[5] Joel Hartman,[5] Allan R. Schmitt[6]

The Kepler mission is monitoring the brightness of ~150,000 stars, searching for evidence of planetary transits. As part of the Hunt for Exomoons with Kepler (HEK) project, we report a planetary system with two confirmed planets and one candidate planet discovered with the publicly available data for KOI-872. Planet b transits the host star with a period P_b = 33.6 days and exhibits large transit timing variations indicative of a perturber. Dynamical modeling uniquely detects an outer nontransiting planet c near the 5:3 resonance (P_c = 57.0 days) with a mass 0.37 times that of Jupiter. Transits of a third planetary candidate are also found: a 1.7–Earth radius super-Earth with a 6.8-day period. Our analysis indicates a system with nearly coplanar and circular orbits, reminiscent of the orderly arrangement within the solar system.

If a planet's orbit is viewed nearly edge-on, the planet may transit over the disk of its host star and periodically block a small fraction of the starlight. The planet's presence is then revealed by a small and repetitive decrease of the host star's brightness during transits. The transit light curve is characterized by the time of transit minimum τ, the transit depth δ, the total duration T_{14}, and the partial duration T_{23} (*1*). A precise measurement of these terms allows an observer to infer the physical properties of the system, such as the radius ratio $p = R_P/R_*$, transit impact parameter b_P, and scaled semimajor axis a_P/R_*, where R_* is the star's physical radius and the P subscript denotes "planet."

For a planet following a strictly Keplerian orbit, the spacing, timing, and other properties of the transit light curve should be unchanging in time. Several effects, however, can produce deviations from the Keplerian case so that the spacing of τ is not strictly periodic and/or T_{14} varies from transit to transit. Such changes are known as transit timing variations (TTVs) and transit duration variations (TDVs), respectively. TTVs are particularly sensitive to gravitational perturbations from additional planets orbiting the host star (*2*–*4*) and distant large moons orbiting the transiting planet (*5*–*7*).

As part of the Hunt for Exomoons with Kepler (HEK) project (*8*), we analyzed the publicly available Kepler data up to Quarter 6 (Q6; released on 7 January 2012). At the time of writing, the 33.6-day-period planetary candidate Kepler-object-of-interest 872.01 (KOI-872.01) is the only known candidate in the system (*9*). The candidate was identified through HEK's target selection procedure as a high-priority object because of the presence of visual transit anomalies and the dynamical capacity to host a moon.

We detrended the raw Kepler photometry of KOI-872, covering 15 transits, using a harmonic filter and an exponential decay ramp correction (*10*). We tested several models to explain the photometry using the multimodal nested sampling algorithm MULTINEST (*11*, *12*), designed to compute the Bayesian evidence for each model.

[1]Department of Space Studies, Southwest Research Institute, Boulder, CO 80302, USA. [2]Harvard-Smithsonian Center for Astrophysics, Cambridge, MA 02138, USA. [3]Niels Bohr Institute, University of Copenhagen, DK-2100 Copenhagen, Denmark. [4]Centre for Star and Planet Formation, Natural History Museum of Denmark, University of Copenhagen, DK-1350 Copenhagen, Denmark. [5]Department of Astrophysical Sciences, Princeton University, Princeton, NJ 05844, USA. [6]Citizen Science.

*To whom correspondence should be addressed. E-mail: davidn@boulder.swri.edu

Supplementary Materials for

Quantum Algorithms for Quantum Field Theories

Stephen P. Jordan,* Keith S. M. Lee, John Preskill

*To whom correspondence should be addressed. E-mail: stephen.jordan@nist.gov

Published 1 June 2012, *Science* **336**, 1130 (2012)
DOI: 10.1126/science.1217069

This PDF file includes:

S.1 Steps of Algorithm and Comments

Our quantum algorithm works by the following sequence of steps.

1. **Prepare the free vacuum.** The free vacuum is a Gaussian superposition, which can be prepared via the method of Kitaev and Webb (*36*). For large $\mathcal{V}$, the dominant cost in Kitaev and Webb's method for producing $\mathcal{V}$-dimensional multivariate Gaussians is the computation of the $\mathbf{LDL}^T$ decomposition of the inverse covariance matrix, where $\mathbf{L}$ is a unit lower triangular matrix, and $\mathbf{D}$ is a diagonal matrix. This can be done in $\tilde{O}(\mathcal{V}^{2.376})$ time with established classical methods (*37, 38*). (The notation $f(n) = \tilde{O}(g(n))$ means $f(n) = O(g(n)\log^c(n))$ for some constant c.) The computation of the matrix elements of the covariance matrix itself is easy because, for large V, the sum

$$G^{(0)}(\mathbf{x}-\mathbf{y}) = \sum_{\mathbf{p}\in\Gamma} L^{-d}\frac{1}{2\omega(\mathbf{p})}e^{i\mathbf{p}\cdot(\mathbf{x}_i-\mathbf{x}_j)} \tag{S1}$$

defining the propagator of the lattice theory is well approximated by an easily evaluated integral.

2. **Excite wavepackets.** The span of $|\mathrm{vac}(0)\rangle|0\rangle$ and $|\psi\rangle|1\rangle$ is an invariant subspace, on which H_ψ acts as

$$H_\psi|\mathrm{vac}(0)\rangle|0\rangle = |\psi\rangle|1\rangle\,, \tag{S2}$$

$$H_\psi|\psi\rangle|1\rangle = |\mathrm{vac}(0)\rangle|0\rangle\,. \tag{S3}$$

Thus,

$$e^{-iH_\psi \pi/2}|\mathrm{vac}(0)\rangle|0\rangle = -i|\psi\rangle|1\rangle\,. \tag{S4}$$

Hence, by simulating a time evolution according to the Hamiltonian H_ψ, we obtain the desired wavepacket state $|\psi\rangle$, up to an irrelevant global phase and extra qubit, which can be discarded. After rewriting H_ψ in terms of the operators $\phi(\mathbf{x})$ and $\pi(\mathbf{x})$, one sees that simulating H_ψ is a very similar task to simulating H and can be done with the same techniques.

The only errors introduced at this step are due to the finite separation distance δ between wavepackets and are of order $\epsilon \sim e^{-m\delta}$. (However, our wavepackets have a constant spread in momentum, and thus differ from the idealization of particles with precisely defined momenta.) The wavepacket preparation thus has complexity scaling linearly with n_{in}, the number of particles being prepared, and necessitates a dependence $V \sim n_{\mathrm{in}} \log^d(1/\epsilon)$.

3. **Adiabatically turn on the interaction.** For $0 \leq s \leq 1$, let

$$H(s) = \sum_{\mathbf{x}\in\Omega} a^d \left[\frac{1}{2}\pi(\mathbf{x})^2 + \frac{1}{2}(\nabla_a\phi)^2(\mathbf{x}) + \frac{1}{2}m_0^2(s)\phi(\mathbf{x})^2 + \frac{\lambda_0(s)}{4!}\phi(\mathbf{x})^4\right] \tag{S5}$$

with $\lambda_0(0) = 0$. U_j is the unitary time evolution induced by $H(t/\tau)$ from $t = \frac{j\tau}{J}$ to $t = \frac{(j+1)\tau}{J}$, namely,

$$U_j \;=\; T\left\{\exp\left[-i\int_{j/J}^{(j+1)/J} H(s)\tau ds\right]\right\}\,, \tag{S6}$$

where $T\{\cdot\}$ indicates the time-ordered product. We suppress the dynamical phases by choosing J to be sufficiently large. The choice of a suitable "path" $(m_0^2(s), \lambda_0(s))$ and the complexity of this state-preparation process depend in a complicated manner on m and λ (§ S.4.1).

4. **Simulate Hamiltonian time evolution.**

5. **Perform Measurements.** There are two possible methods, described below.

   i) Adiabatically turn off the interaction and measure occupation numbers of momentum modes. This method is suitable if there are no outgoing bound states. The adiabatic turn-off of the coupling is simply the time-reversed version of the adiabatic turn-on. For a given $\mathbf{p}$, measurement of $L^{-d}a^\dagger_{\mathbf{p}}a_{\mathbf{p}}$ by phase estimation can be implemented with $O\left(\mathcal{V}^{2+\frac{1}{2k}}\right)$ quantum gates via a k^{th}-order Suzuki-Trotter formula. Furthermore, if we instead simulate localized detectors, the computational cost becomes independent of V (much as the computational cost of creating local wavepackets is independent of V), but the momentum resolution becomes lower, as dictated by the uncertainty principle.

   ii) Divide space into small regions, and measure the total energy and momentum operators in each one via phase estimation. Details are given in Sec. S.6.

The allowable rate of adiabatic increase of the coupling constant during state preparation is determined by the physical mass of the theory. In the weakly coupled case, this can be calculated perturbatively. In the strongly coupled case, it is not known how to do the calculation. Thus one is left with the problem of determining how fast one can perform the adiabatic state preparation without introducing errors. Fortunately, one can easily calculate the mass using a quantum computer, as follows. First, one adiabatically prepares the interacting vacuum state at some small λ_0 and measures the energy of the vacuum using phase estimation. The speed at which to increase λ_0 can be chosen perturbatively for this small value of λ_0. Next, one adiabatically prepares the state with a single zero-momentum particle at the same value of λ_0 and measures its energy using phase estimation. Taking the difference of these values yields the physical mass. This value of the physical mass provides guidance as to the speed of adiabatic increase of the coupling to reach a slightly higher λ_0. Repeating this process for successively higher λ_0

allows one to reach strong coupling, while always having an estimate of the mass by which to choose a safe speed for adiabatic state preparation. In addition, mapping out the physical mass as a function of bare parameters (hence, for example, mapping out the phase diagram) may be of independent interest.

S.2 Efficiency

In the weakly coupled case, it is interesting to analyze complexity as a function of precision, because the high-precision limit is inaccessible via classical methods such as Feynman diagrams. We bound errors from spatial discretization by demanding that physical observables such as scattering cross sections be accurate to within a factor of $1 + \epsilon$. The other sources of error can be bounded even more stringently: we can ensure that the induced total variation distance between the simulated and exact probability distributions is bounded by ϵ. In a theory with a non-zero mass, errors due to imperfect particle separation in the in and out states shrink exponentially with distance. Thus, V needs to scale only polylogarithmically with ϵ. Similarly, by the analysis of § S.4, the number of qubits per site scales only logarithmically with ϵ. By Eq. S110, the errors resulting from use of a k^{th}-order Suzuki-Trotter formula with n timesteps are $\epsilon \sim n^{-2k}$. Thus, the complexity scales as $\epsilon^{-1/2k}$. For large k, the dominant contributions to scaling with ϵ are spatial discretization and imperfect adiabaticity.

The effect of spatial discretization is captured by (infinitely many) additional terms in the effective Hamiltonian. Truncation of these terms alters the calculated probability of scattering events. In particular, the two dominant extra terms in the effective Hamiltonian are $\sum_i \phi \partial_i^4 \phi$ and ϕ^6 terms, arising from discretization of $(\nabla_a \phi)^2$ and quantum effects, respectively. The coefficient of the $\sum_i \phi \partial_i^4 \phi$ term is $O(a^2)$, and the coefficient of the ϕ^6 term is $O(a^{5-d})$, so that the former dominates for $d = 1, 2$, whereas the latter makes a comparable contribution for

$d = 3$. Thus, the overall discretization error is

$$\epsilon = O(a^2)\,, \quad d = 1, 2, 3\,. \tag{S7}$$

(To improve the scaling, one can use better finite differences to approximate the derivative, and/or include the ϕ^6 operator. However, renormalization and mixing of the coefficients make this idea more complicated than it is in standard numerical analysis.)

The diabatic errors at weak coupling are estimated and summarized in § S.4.1.1. The errors are quantified by a probability ϵ of observing stray particles. Substituting the $a \sim \sqrt{\epsilon}$ dependence from Eq. S7 into Eq. S95 yields[1]

$$G_{\text{adiabatic}} \sim \left(\frac{1}{\epsilon}\right)^{1+d/2+o(1)}, \quad d = 1, 2, 3 \tag{S8}$$

scaling for the adiabatic state preparation. We use little-o notation to convey precisely that we are neglecting both logarithmic factors and contributions to the exponent that become arbitrarily small as we use higher-order Suzuki-Trotter formulae. The other slow part of the algorithm is the preparation of the free vacuum. This scales as

$$G_{\text{prep}} = \tilde{O}(\mathcal{V}^{2.376}) = \tilde{O}(a^{-2.376d}) = \tilde{O}(\epsilon^{-1.188d})\,, \tag{S9}$$

where the last equality follows from Eq. S7. Thus, in $d = 1, 3$ the adiabatic state preparation is the dominant cost, whereas in $d = 2$ the preparation of the free vacuum dominates. This leaves a final asymptotic scaling of

$$G_{\text{total}} = O(G_{\text{adiabatic}} + G_{\text{prep}}) \sim \begin{cases} \left(\frac{1}{\epsilon}\right)^{1.5+o(1)}, & d = 1, \\ \left(\frac{1}{\epsilon}\right)^{2.376+o(1)}, & d = 2, \\ \left(\frac{1}{\epsilon}\right)^{5.5+o(1)}, & d = 3. \end{cases} \tag{S10}$$

The number of quantum gates used to simulate the strongly coupled theory has scaling in $1/(\lambda_c - \lambda_0)$ and p that is dominated by adiabatic state preparation (§ S.4.2). We also estimate

[1] Whether we use Eq. S95 or Eq. S96 affects only the scaling with V.

scaling with n_{out} as follows. For two incoming particles with momenta $\mathbf{p}$ and $-\mathbf{p}$, the maximum number of kinematically allowed outgoing particles is $n_{\text{out}} \sim p$. For continuum behavior, $p = \eta/a$ for constant $\eta \ll 1$. Furthermore, one needs $V \sim n_{\text{out}}$ to obtain good asymptotic out states separated by a distance of order at least $1/m_0$. Thus, $\mathcal{V} \sim n_{\text{out}}^{d+1}$, so one needs $n_{\text{out}}^{2.376(d+1)}$ gates to prepare the free vacuum and, by Eq. S107, $n_{\text{out}}^{2d+3+o(1)}$ gates to reach the interacting theory adiabatically. (The adiabatic turn-off takes no longer than the adiabatic turn-on.) Hence the total scaling in n_{out} is dominated by preparation of the free vacuum in three-dimensional spacetime, but by adiabatic turn-on in two-dimensional spacetime. These results are summarized in Table 1 of the main text.

S.3 Mass Renormalization

The physical, or renormalized, mass as a function of the coupling features prominently in our calculations. For the weak-coupling regime, its form is obtained by perturbation theory. For the strong-coupling regime, we use its known behavior near the phase transition.

At first order in the coupling, the shift of the squared mass is given by i times the one-loop Feynman diagram

. (S11)

At second order, there is also a contribution from the two-loop diagram

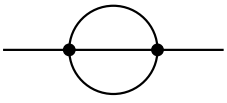

. (S12)

The calculation of these diagrams is quite analogous to standard calculations in perturbative quantum field theory, but there are a couple of differences. First, the propagator is different because of the discretization. Secondly, integrals over components $1, \ldots, d$ (but not component 0) of loop momenta are cut off by π/a; in other words, the lattice spacing acts as an ultraviolet

regulator. These differences alter the nature of the integrals and hence what methods can be used to evaluate them.

The existence of a phase transition in the ϕ^4 theory in $D = 2$ or 3 spacetime dimensions was shown rigorously in (*8–10*). As the system approaches it, thermodynamic functions and correlation functions exhibit power-law behavior, as is characteristic of a second-order phase transition. In particular, for constant m_0^2,

$$m \sim |\lambda_0 - \lambda_c|^\nu \,, \tag{S13}$$

where λ_c, the critical value of the coupling, depends on m_0^2.

Empirically, it has been found that systems with second-order phase transitions can be classified into universality classes. Within each class, critical exponents are universal, taking the same values for all systems. (This universality is explained by the concept of the renormalization group.) The ϕ^4 theory is believed to be in the same universality class as the Ising model, for which

$$\nu = \begin{cases} 1\,, & D = 2\,, \\ 0.63\ldots\,, & D = 3\,. \end{cases} \tag{S14}$$

The value above for $D = 3$ has also been obtained directly in the ϕ^4 theory by Borel resummation (*43*).

In $D = 4$ dimensions, in contrast, the believed triviality of the continuum ϕ^4 theory implies that there is no non-trivial fixed point of the renormalization group and hence no phase transition as one varies (m_0^2, λ_0). Moreover, triviality places bounds on the maximum value of the renormalized coupling (*44*). In particular, strong coupling requires pa to be $O(1)$: in the continuum-like regime, renormalized perturbation theory should be valid.

S.4 Representation by Qubits

The required number of qubits per site is

$$n_b = \lceil \log_2 (1 + 2\phi_{\max}/\delta_\phi) \rceil \,. \tag{S15}$$

In this section we show that one can simulate processes at energy scale E, while maintaining $1 - \epsilon_{\rm trunc}$ inner product with the exact state, with n_b logarithmic in $1/a$, $1/\epsilon_{\rm trunc}$, and V. Our analysis is non-perturbative, and thus applies equally to strongly and weakly coupled ϕ^4 theory.

Let $|\psi\rangle$ be the state, expressed in the field representation, namely,

$$|\psi\rangle = \int_{-\infty}^{\infty} d\phi_1 \cdots \int_{-\infty}^{\infty} d\phi_{\mathcal{V}}\ \psi(\phi_1, \ldots, \phi_{\mathcal{V}}) |\phi_1, \ldots, \phi_{\mathcal{V}}\rangle \,, \tag{S16}$$

and let

$$|\psi_{\rm cut}\rangle = \int_{-\phi_{\max}}^{\phi_{\max}} d\phi_1 \cdots \int_{-\phi_{\max}}^{\phi_{\max}} d\phi_{\mathcal{V}}\ \psi(\phi_1, \ldots, \phi_{\mathcal{V}}) |\phi_1, \ldots \phi_{\mathcal{V}}\rangle \,. \tag{S17}$$

Then

$$\langle \psi | \psi_{\rm cut} \rangle = \int_{-\phi_{\max}}^{\phi_{\max}} d\phi_1 \cdots \int_{-\phi_{\max}}^{\phi_{\max}} d\phi_{\mathcal{V}}\ \rho(\phi_1, \ldots, \phi_{\mathcal{V}}) \,, \tag{S18}$$

where ρ is the probability distribution

$$\rho(\phi_1, \ldots, \phi_{\mathcal{V}}) = |\psi(\phi_1, \ldots, \phi_{\mathcal{V}})|^2 \,. \tag{S19}$$

In other words, $\langle \psi | \psi_{\rm cut} \rangle = 1 - p_{\rm out}$, where $p_{\rm out}$ is the probability that at least one of $\phi_1, \ldots, \phi_{\mathcal{V}}$ is out of the range $[-\phi_{\max}, \phi_{\max}]$. By the union bound ($\Pr(A \cup B) \le \Pr(A) + \Pr(B)$),

$$\langle \psi | \psi_{\rm cut} \rangle \ge 1 - \mathcal{V} \max_{\mathbf{x} \in \Omega} p_{\rm out}(\mathbf{x}) \,, \tag{S20}$$

where $p_{\rm out}(\mathrm{x})$ is the probability that $\phi(\mathbf{x})$ is out of the range $[-\phi_{\max}, \phi_{\max}]$.

Let $\mu_{\phi(\mathbf{x})}$ and $\sigma_{\phi(\mathbf{x})}$ denote the mean and standard deviation of $\phi(\mathbf{x})$ determined by ρ. By Chebyshev's inequality, choosing $\phi_{\max} = \mu_{\phi(\mathbf{x})} + c\sigma_{\phi(\mathbf{x})}$ ensures

$$p_{\rm out}(\mathbf{x}) \le \frac{1}{c^2} \,. \tag{S21}$$

Thus, choosing

$$\phi_{\max} = O\left(\max_{\mathbf{x}\in\Omega}\left(\mu_{\phi(\mathbf{x})} + \sqrt{\frac{\mathcal{V}}{\epsilon_{\rm trunc}}}\sigma_{\phi(\mathbf{x})}\right)\right) \tag{S22}$$

ensures $\langle\psi|\psi_{\rm cut}\rangle \geq 1 - \epsilon_{\rm trunc}$.

Next, we observe the following, which is straightforward to prove.

Proposition 1 *Let $\hat{p}$ and $\hat{q}$ be Hermitian operators on $L^2(\mathbb{R})$ obeying the canonical commutation relation $[\hat{q},\hat{p}] = i\mathbb{1}$. Then the eigenbasis of $\hat{p}$ is the Fourier transform of the eigenbasis of $\hat{q}$.*

By Proposition 1, the eigenbasis of $a^d\pi(\mathbf{x})$ is the Fourier transform of the eigenbasis of $\phi(\mathbf{x})$. Thus, discretizing $\phi(\mathbf{x})$ in increments of $\delta_{\phi(\mathbf{x})}$ is roughly equivalent to the truncation $-\pi_{\max} \leq \pi(\mathbf{x}) \leq \pi_{\max}$, where

$$\pi_{\max} \sim \frac{1}{a^d\delta_{\phi(\mathbf{x})}}\,. \tag{S23}$$

By the same argument used to choose $\phi_{\max}$, choosing

$$\pi_{\max} = O\left(\max_{\mathbf{x}\in\Omega}\left(\mu_{\pi(\mathbf{x})} + \sigma_{\pi(\mathbf{x})}\sqrt{\frac{\mathcal{V}}{\epsilon_{\rm trunc}}}\right)\right) \tag{S24}$$

ensures fidelity $1 - \epsilon_{\rm trunc}$ between $|\psi\rangle$ and its truncated and discretized version.

To obtain useful bounds on $\phi_{\max}$ and $\pi_{\max}$, we must bound $\mu_{\phi(\mathbf{x})}$, $\sigma_{\phi(\mathbf{x})}$, $\mu_{\pi(\mathbf{x})}$, and $\sigma_{\pi(\mathbf{x})}$. To this end, we make the following straightforward observation.

Proposition 2 *Let M be a Hermitian operator and let $|\psi\rangle$ be a quantum state. Then $|\langle\psi|M|\psi\rangle| \leq \sqrt{\langle\psi|M^2|\psi\rangle}$.*

Applied to the definitions

$$\mu_{\phi(\mathbf{x})} = \langle\psi|\phi(\mathbf{x})|\psi\rangle\,, \tag{S25}$$

$$\sigma_{\phi(\mathbf{x})} = \sqrt{\langle\psi|\phi(\mathbf{x})^2|\psi\rangle - \langle\psi|\phi(\mathbf{x})|\psi\rangle^2}\,, \tag{S26}$$

$$\mu_{\pi(\mathbf{x})} = \langle\psi|\pi(\mathbf{x})|\psi\rangle\,, \tag{S27}$$

$$\sigma_{\pi(\mathbf{x})} = \sqrt{\langle\psi|\pi(\mathbf{x})^2|\psi\rangle - \langle\psi|\pi(\mathbf{x})|\psi\rangle^2}\,, \tag{S28}$$

Proposition 2 implies that $\mu_{\phi(\mathbf{x})}$ and $\sigma_{\phi(\mathbf{x})}$ are each at most $\sqrt{\langle\psi|\phi(\mathbf{x})^2|\psi\rangle}$, and $\mu_{\pi(\mathbf{x})}$ and $\sigma_{\pi(\mathbf{x})}$ are each at most $\sqrt{\langle\psi|\pi(\mathbf{x})^2|\psi\rangle}$. Thus, by Eq. S22 and Eq. S24,

$$\phi_{\max} = O\left(\max_{\mathbf{x}\in\Omega}\sqrt{\frac{\mathcal{V}}{\epsilon_{\text{trunc}}}\langle\psi|\phi(\mathbf{x})^2|\psi\rangle}\right), \tag{S29}$$

$$\pi_{\max} = O\left(\max_{\mathbf{x}\in\Omega}\sqrt{\frac{\mathcal{V}}{\epsilon_{\text{trunc}}}\langle\psi|\pi(\mathbf{x})^2|\psi\rangle}\right), \tag{S30}$$

so that, by Eq. S15 and Eq. S23,

$$n_b = O\left(\log_2\left(a^d\frac{\mathcal{V}}{\epsilon_{\text{trunc}}}\max_{\mathbf{x},\mathbf{y}\in\Omega}\sqrt{\langle\psi|\pi(\mathbf{x})^2|\psi\rangle\langle\psi|\phi(\mathbf{y})^2|\psi\rangle}\right)\right). \tag{S31}$$

To establish logarithmic scaling of n_b, we need only prove polynomial upper bounds on $\langle\psi|\phi(\mathbf{x})^2|\psi\rangle$ and $\langle\psi|\pi(\mathbf{x})^2|\psi\rangle$. Rather than making a physical estimate of these expectation values, we prove simple upper bounds that are probably quite loose. In the adiabatic state preparation described in § S.4.1, the parameters m_0^2 and λ_0 are varied. The following two propositions cover all the combinations of parameters used in the adiabatic preparation and subsequent scattering of both strongly and weakly coupled wavepackets.

Proposition 3 *Let H be of the form shown in Eq. S5. Suppose $m_0^2 > 0$ and $\lambda_0 \geq 0$. Let $|\psi\rangle$ be any state of the field such that $\langle\psi|H|\psi\rangle \leq E$. Then $\forall\mathbf{x}\in\Omega$,*

$$\langle\psi|\phi(\mathbf{x})^2|\psi\rangle \leq \frac{2E}{a^d m_0^2}, \tag{S32}$$

$$\langle\psi|\pi(\mathbf{x})^2|\psi\rangle \leq \frac{2E}{a^d}. \tag{S33}$$

Proof:

$$E \geq \langle\psi|H|\psi\rangle \tag{S34}$$

$$= \langle\psi|\sum_{\mathbf{y}\in\Omega}a^d\left[\frac{1}{2}\pi(\mathbf{y})^2 + \frac{1}{2}(\nabla_a\phi)^2(\mathbf{y}) + \frac{m_0^2}{2}\phi(\mathbf{y})^2 + \frac{\lambda_0}{4!}\phi(\mathbf{y})^4\right]|\psi\rangle \tag{S35}$$

$$\geq \langle\psi|a^d\frac{m_0^2}{2}\phi(\mathbf{x})^2|\psi\rangle, \tag{S36}$$

where the last inequality follows because all of the operators we have dropped are positive semidefinite. This establishes Eq. S32. Similarly, we can drop all but the $\pi(\mathbf{x})$ term from the right-hand side of Eq. S35, leaving

$$E \geq \langle\psi| a^d \frac{1}{2} \pi(\mathbf{x})^2 |\psi\rangle \,, \tag{S37}$$

which establishes Eq. S33. □

Proposition 4 *Let H be of the form shown in Eq. S5. Suppose $m_0^2 \leq 0$ and $\lambda_0 > 0$. Let $|\psi\rangle$ be any state of the field such that $\langle\psi|H|\psi\rangle \leq E$. Then $\forall \mathbf{x} \in \Omega$,*

$$\langle\psi|\phi(\mathbf{x})^2|\psi\rangle \;\leq\; -\frac{24m_0^2}{\lambda_0} + \sqrt{\frac{36m_0^4}{\lambda_0^2} + \frac{24}{\lambda_0 a^d}\left(E + \frac{3(V-a^d)m_0^4}{2\lambda_0}\right)}\,, \tag{S38}$$

$$\langle\psi|\pi(\mathbf{x})^2|\psi\rangle \;\leq\; \frac{2}{a^d}\left(E + \frac{3Vm_0^4}{2\lambda_0}\right)\,, \tag{S39}$$

where V is the physical volume.

Proof: The operator

$$U(\mathbf{x}) = \frac{m_0^2}{2}\phi(\mathbf{x})^2 + \frac{\lambda_0}{4!}\phi(\mathbf{x})^4 \tag{S40}$$

is sufficiently simple that we can directly calculate its minimal eigenvalue $U_{\min}$. If $m_0^2 \leq 0$ and $\lambda > 0$, then

$$U_{\min} = -\frac{3m_0^4}{2\lambda_0}\,. \tag{S41}$$

Thus, for *any* state $|\psi\rangle$,

$$\langle\psi| \sum_{\mathbf{x}\in\Omega} a^d U(\mathbf{x}) |\psi\rangle \geq \frac{-3Vm_0^4}{2\lambda_0}\,. \tag{S42}$$

Hence, recalling Eq. S5, we obtain

$$\begin{aligned} E &\geq \langle\psi|H|\psi\rangle && \text{(S43)} \\ &= \langle\psi| \sum_{\mathbf{y}\in\Omega} a^d \left[\frac{1}{2}\pi(\mathbf{y})^2 + \frac{1}{2}(\nabla_a\phi)^2(\mathbf{y}) + \frac{m_0^2}{2}\phi(\mathbf{y})^2 + \frac{\lambda_0}{4!}\phi(\mathbf{y})^4\right] |\psi\rangle && \text{(S44)} \\ &\geq \langle\psi| \sum_{\mathbf{y}\in\Omega} a^d \left[\frac{1}{2}\pi(\mathbf{y})^2 + \frac{1}{2}(\nabla_a\phi)^2(\mathbf{y})\right] |\psi\rangle - \frac{3Vm_0^4}{2\lambda_0} && \text{(S45)} \\ &\geq \langle\psi| \frac{a^d}{2}\pi(\mathbf{x})^2|\psi\rangle - \frac{3Vm_0^4}{2\lambda_0}\,. && \text{(S46)} \end{aligned}$$

Eq. S45 follows from Eq. S42. Eq. S46 holds (for any choice of $\mathbf{x}$) because all of the operators we have dropped are positive semidefinite. This establishes Eq. S39.

Similarly, dropping positive operators from Eq. S44 and using Eq. S42 yield, for any $\mathbf{x}$,

$$a^d\langle\psi| \left(\frac{m_0^2}{2}\phi(\mathbf{x})^2 + \frac{\lambda_0}{4!}\phi(\mathbf{x})^4\right) |\psi\rangle \leq \left(E + \frac{3(V-a^d)m_0^4}{2\lambda_0}\right)\,. \tag{S47}$$

Applying Proposition 2 with $M = \phi(\mathbf{x})^2$ shows that $\langle\psi|\phi(\mathbf{x})^4|\psi\rangle \geq \langle\psi|\phi(\mathbf{x})^2|\psi\rangle^2$. Thus,

$$a^d \left[\frac{m_0^2}{2}\langle\psi|\phi(\mathbf{x})^2|\psi\rangle + \frac{\lambda_0}{4!}\langle\psi|\phi(\mathbf{x})^2|\psi\rangle^2\right] \leq \left(E + \frac{3(V-a^d)m_0^4}{2\lambda_0}\right)\,. \tag{S48}$$

Via the quadratic formula, this implies Eq. S38. □

S.4.1 Adiabatic Preparation of Interacting Wavepackets

In this section, we analyze the adiabatic state-preparation procedure. To analyze the error due to finite τ and J, we consider the process of preparing a single-particle wavepacket. The procedure performs similarly in preparing wavepackets for multiple particles, provided the particles are separated by more than the characteristic length $1/m$ of the interaction. In what follows we use $p = |\mathbf{p}|$, rather than the D-vector, as will be clear from the context.

The phase induced by M_j in the momentum-p eigenstate of $H(s)$ (with energy $E_p(s)$) is

$$\theta_j(p) = \left(E_p\left(\frac{j+1}{J}\right) + E_p\left(\frac{j}{J}\right)\right)\frac{\tau}{2J} - \tau\int_{j/J}^{(j+1)/J} ds E_p(s)\,. \tag{S49}$$

Taylor expanding E_p about $s = (j + \frac{1}{2})/J$ yields

$$\theta_j(p) = \frac{\tau}{12J^3}\frac{\partial^2 E_p}{\partial s^2} + O(J^{-5})\,. \tag{S50}$$

Thus, the total phase induced is

$$\begin{aligned}\theta(p) &= \sum_{j=0}^{J-1}\theta_j(p) &\text{(S51)}\\ &\simeq \frac{\tau}{12J^2}\int_0^1 ds\frac{\partial^2 E_p}{\partial s^2} &\text{(S52)}\\ &= \frac{\tau}{12J^2}\left.\frac{\partial E_p}{\partial s}\right|_0^1, &\text{(S53)}\end{aligned}$$

where the approximation holds for large J. For a Lorentz-invariant theory, $E_p(s)$ must take the form

$$E_p(s) = \sqrt{p^2 + m^2(s)}\,. \tag{S54}$$

This should be a good approximation for the lattice theory provided the particle momentum satisfies $p \ll 1/a$. Substituting Eq. S54 into Eq. S53 yields

$$\theta(p) \simeq \frac{\tau}{24J^2}\left.\frac{\frac{\partial m^2(s)}{\partial s}}{\sqrt{p^2 + m^2(s)}}\right|_0^1. \tag{S55}$$

Next, we consider the effect of this phase shift on a wavepacket centered around momentum $\bar{p}$. If the wavepacket is narrowly concentrated in momentum, then we can Taylor expand $\theta(p)$ to first order about $\bar{p}$:

$$\theta(p) \simeq \theta(\bar{p}) + \mathcal{D}\cdot(p - \bar{p})\,, \tag{S56}$$

where

$$\mathcal{D} = \left.\frac{\partial\theta}{\partial p}\right|_{\bar{p}}, \tag{S57}$$

The phase shift $e^{i\mathcal{D}\cdot(p-\bar{p})}$ induces a translation (in position space) of any wavepacket by a distance $\mathcal{D}$. From Eq. S57 and Eq. S55, we have

$$\mathcal{D} \simeq \frac{\tau\bar{p}}{24J^2}\left.\frac{\frac{\partial m^2(s)}{\partial s}}{\left(\bar{p}^2 + m^2(s)\right)^{3/2}}\right|_{s=0}^{s=1}. \tag{S58}$$

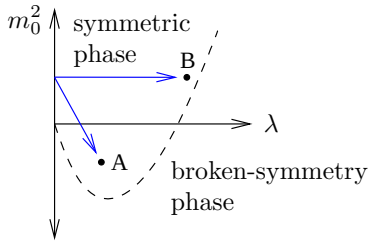

Figure S1: The dashed line illustrates schematically the location of a quantum phase transition of ϕ^4 theory in two and three spacetime dimensions. A and B denote weakly and strongly coupled continuum-like theories, respectively. We prepare them adiabatically by following the arrows starting from the massive free theory ($m_0^2 > 0$, $\lambda_0 = 0$). To maintain adiabaticity the path must not cross the quantum phase transition.

We next determine the complexity by demanding that the propagation length $\mathcal{D}$ be restricted to some small constant, and that the probability of diabatic particle creation be small. Together, these criteria determine J and τ. We can obtain a tighter bound in the perturbative case than in the general case, so we treat these separately.

S.4.1.1 Weak Coupling

We wish to prepare the weakly coupled continuum-like theory by adiabatically following a path that does not cross the quantum phase transition, as illustrated in Fig. S1. Note that, in the weakly coupled continuum limit $a \to 0$, m_0^2 is negative. The path illustrated in Fig. S1 can be described by the following parametrization of $H(s)$ from Eq. S5:

$$m_0^2(s) = m^2 + s\delta_m \,, \tag{S59}$$

$$\lambda_0(s) = s\lambda_0 \,. \tag{S60}$$

Let $m(s)$ denote the physical mass of particles defined by $H(s)$. By Eq. S59 and Eq. S60, $m_0(0) = m(0) = m$. We choose δ_m so that $m(1)$ is also equal to m. Thus, $H(s)$ linearly interpolates between a non-interacting theory with physical mass m and an interacting theory with physical mass m.

We wish to find the asymptotic scaling of the run time of the adiabatic state preparation. The question is, with which parameter should we consider scaling? There are at least three regimes in which classical methods for computing scattering amplitudes break down or are inefficient: strong coupling, large numbers of external particles, and high precision. In this section we are considering only weak coupling (that is, $\lambda/m^{4-D} \ll 1$), leaving discussion of strong coupling until the next section. For an asymptotically large number of external particles, the efficiency of our algorithm depends upon strong coupling, for the following reason. A connected Feynman diagram involving n external particles must have at least $v = O(n)$ vertices, so the amplitude for such a process is suppressed by a factor of $\left(\frac{\lambda}{E^{4-D}}\right)^v$, where E is the energy scale of the process. Since $E \geq m$, many-particle scattering events are exponentially rare at weak coupling and thus cannot be efficiently observed in experiments or simulations. This leaves the high-precision frontier. Recall that the perturbation series used in quantum field theory are asymptotic but not convergent. Thus, perturbative methods cannot be extended to arbitrarily high precision.

Hence, in this section we consider the quantum gate complexity of achieving arbitrarily high precision. To do so, one chooses a small to obtain small discretization errors, V large to obtain better particle separation, τ long to improve adiabaticity, and J large enough to limit particle propagation as the interaction is turned on. Thus, we wish to know the scaling of the probability of particle creation from the vacuum (denoted P_{create}) with a, V, τ, and J. In this context, we consider m, λ, and the incoming momentum to be constants.

We now analyze $m^2(s)$ (to second order in λ_0), which determines the energy gap along the adiabatic path and the propagation of wavepackets. Evaluating diagrams S11 and S12 yields

$$m^2(s) = m_0^2(s) + s\lambda_0\mu^{(1)} + s^2\lambda_0^2\mu^{(2)} + O(\lambda_0^3)\,, \tag{S61}$$

where

$$\mu^{(1)} = \begin{cases} \frac{1}{8\pi} \log\left(\frac{64}{m^2 a^2}\right) , & d = 1, \\ \frac{r_0^{(2)}}{16\pi^2} \frac{1}{a} , & d = 2, \\ \frac{r_0^{(3)}}{32\pi^3} \frac{1}{a^2} , & d = 3, \end{cases} \tag{S62}$$

and

$$\mu^{(2)} = \begin{cases} -\frac{1}{384 m^2} , & d = 1, \\ \frac{1}{96\pi^2} \log(ma) , & d = 2, \\ -\frac{r_1^{(3)}}{1536\pi^7} \frac{1}{a^2} , & d = 3. \end{cases} \tag{S63}$$

Here, $r_0^{(2)}$, $r_0^{(3)}$, and $r_1^{(3)}$ are numerical constants. Thus,

$$\delta_m = -\lambda_0 \mu^{(1)} - \lambda_0^2 \mu^{(2)} + O(\lambda_0^3). \tag{S64}$$

Substituting Eq. S64 and Eq. S59 into Eq. S61 yields

$$m^2(s) = m^2 + s(s-1)\lambda_0^2 \mu^{(2)} + O(\lambda_0^3) \,. \tag{S65}$$

For the purpose of analyzing adiabaticity, we note that

$$\min_{0 \le s \le 1} m^2(s) = m^2 + O(\lambda_0^3) \,. \tag{S66}$$

This feature is helpful, because a small mass gap would necessitate slow adiabatic preparation. To analyze wavepacket propagation, we substitute Eq. S65 into Eq. S58, and obtain

$$\begin{aligned} \mathcal{D} &= \frac{\tau \bar{p}}{24 J^2} \frac{(2s-1)\lambda_0^2 \mu^{(2)}}{(\bar{p}^2 + m^2)^{3/2}} \Bigg|_{s=0}^{s=1} \\ &= \frac{\tau \bar{p}}{12 J^2} \frac{\lambda_0^2 \mu^{(2)}}{(\bar{p}^2 + m^2)^{3/2}} . \end{aligned} \tag{S67}$$

We can solve Eq. S67 to determine the necessary scaling of J. We are primarily interested in the scaling of J with a, because we wish to investigate the high-precision limit. Making the simplifying assumption that the particles are highly relativistic ($\bar{p}^2 \gg m^2$), we have

$$J \simeq \sqrt{\frac{\tau \lambda_0^2 \mu^{(2)}}{12 \mathcal{D} \bar{p}^2}} \,. \tag{S68}$$

Substituting Eq. S63 into Eq. S68 yields

$$J = \begin{cases} \tilde{O}\left(\sqrt{\frac{\tau\lambda_0^2}{m^2\mathcal{D}\bar{p}^2}}\right), & d = 1, \\ \tilde{O}\left(\sqrt{\frac{\tau\lambda_0^2}{\mathcal{D}\bar{p}^2}}\right), & d = 2, \\ \tilde{O}\left(\sqrt{\frac{\tau\lambda_0^2}{a^2\mathcal{D}\bar{p}^2}}\right), & d = 3. \end{cases} \tag{S69}$$

To determine τ, we next consider adiabaticity. Let $H(s)$ be any Hamiltonian differentiable with respect to s. Let $|\phi_l(s)\rangle$ be an eigenstate $H(s)|\phi_l(s)\rangle = E_l(s)|\phi_l(s)\rangle$ separated by a non-zero energy gap for all s. Let $|\psi_l(t)\rangle$ be the state obtained by Schrödinger time evolution according to $H(t/\tau)$ with initial condition $|\psi_l(0)\rangle = |\phi_l(0)\rangle$. The diabatic transition amplitude to any other eigenstate $H(s)|\phi_k(s)\rangle = E_k(s)|\phi_k(s)\rangle$ ($k \neq l$) is (*45*)

$$\langle\phi_k(s)|\psi_l(\tau s)\rangle \sim \int_0^s d\sigma \frac{\langle\phi_k(\sigma)|\frac{dH}{ds}|\phi_l(\sigma)\rangle}{E_l(\sigma) - E_k(\sigma)} e^{i\tau(\varphi_k(\sigma)-\varphi_l(\sigma))} \left(1 + O(1/\tau)\right) . \tag{S70}$$

(The integrand is made well-defined by the phase convention $\langle\phi_k|\frac{d|\phi_k\rangle}{ds} = 0$.) Here,

$$\varphi_l(s) = \int_0^s d\sigma E_l(\sigma) . \tag{S71}$$

In the case that E_l, E_k, and $\langle\phi_k|\frac{dH}{ds}|\phi_l\rangle$ are s-independent, this integral gives

$$\langle\phi_k(s)|\psi_l(\tau s)\rangle \sim \left(1 - e^{i\tau(E_k-E_l)s}\right) \frac{\langle\phi_k|\frac{dH}{ds}|\phi_l\rangle}{-i\tau(E_k - E_l)^2}(1 + O(1/\tau)) . \tag{S72}$$

In the case that these quantities are approximately s-independent, Eq. S72 should hold as an approximation. The quadratic dependence on $E_k - E_l$ is an adiabatic approximation traditionally used in physics. Motivated by applications in quantum computation, mathematicians have developed bounds that hold rigorously even with strong s dependence (*46*). These more general results have a less favorable (cubic) dependence on $E_k - E_l$. However, the traditional adiabatic approximation appears to be applicable to our analysis.

In reality, we wish to prepare a wavepacket state, not an eigenstate. However, the wavepacket is well separated from other particles and narrowly concentrated in momentum space. Thus, we

shall approximate it by an eigenstate $|\phi_l(s)\rangle$. Furthermore, by our choice of path, the energy gap is kept constant to first order in the coupling, and thus Eq. S72 should be a good approximation to Eq. S70.

Summing the transition amplitudes to some state $|\phi_k\rangle$ from the J steps in in our preparation process and applying the triangle inequality[2] yield the following:

$$|\langle\phi_k|\psi_l(\tau)\rangle| = O\left(\frac{1}{\tau}\sum_{j=0}^{J}\left|\frac{\langle\phi_k(j/J)|\frac{dH}{ds}|\phi_l(j/J)\rangle}{(E_k(j/J)-E_l(j/J))^2}\right|\right) . \tag{S73}$$

The $j = 0$ term in this sum can be evaluated exactly, because it arises from the free theory. At $j \neq 0$ the theory is no longer exactly solvable. However, one obtains the lowest-order contribution to the matrix element $\langle \mathbf{p}_1, \mathbf{p}_2, \mathbf{p}_3, \mathbf{p}_4; s = 1|\phi^4|\mathrm{vac}(1)\rangle$ in renormalized perturbation theory simply by taking the $j = 0$ expression and replacing m_0 with the physical mass and λ_0 with the physical coupling. Our adiabatic path, Eq. S59, is designed so that the physical mass at $s = 1$ matches the bare mass at $j = 0$. Furthermore, the physical coupling differs from the bare coupling only by a logarithmically divergent (in a) correction for $d = 3$ and non-divergent corrections for $d = 1, 2$.[3] Thus, we can make the following approximation:

$$|\langle\phi_k|\psi_l(\tau)\rangle| = \tilde{O}\left(\frac{J}{\tau}\left|\frac{\langle\phi_k(0)|\frac{dH}{ds}|\phi_l(0)\rangle}{(E_k(0)-E_l(0))^2}\right|\right) . \tag{S74}$$

Diabatic errors come in two types, creation of particles from the vacuum and splitting of the incoming particles. The matrix element in the numerator of Eq. S74 can correspondingly be decomposed as the sum of two contributions. We first consider particle creation from the vacuum, taking $|\phi_l(s)\rangle$ to be $|\mathrm{vac}(s)\rangle$.

[2]The $O(J)$ scaling obtained by the triangle inequality can be confirmed by a more detailed calculation taking into account the relative phases of the contributions to the total transition amplitude.

[3]Carrying out the necessary calculations, one finds

$$\lambda \;=\; \begin{cases} \lambda_0 - \frac{3\lambda_0^2}{8\pi(m^{(1)})^2} + \cdots , & \text{for } d = 1, \\ \lambda_0 - \frac{3\lambda_0^2}{16\pi m^{(1)}} + \cdots , & \text{for } d = 2, \\ \lambda_0 + \frac{3\lambda_0^2}{16\pi^2}\log(m^{(1)}a) + \cdots , & \text{for } d = 3. \end{cases}$$

By Eq. S59 and Eq. S60,

$$\frac{dH}{ds} = \sum_{\mathbf{x}\in\Omega} a^d \left[\frac{\lambda_0}{4!}\phi^4(\mathbf{x}) + \frac{1}{2}\delta_m\phi^2(\mathbf{x})\right]. \tag{S75}$$

Substituting this into the numerator of Eq. S74, setting $|\phi_l(0)\rangle = |\mathrm{vac}(0)\rangle$, and expanding ϕ in terms of creation and annihilation operators show that the only potentially non-zero transition amplitudes are to states $|\phi_k(0)\rangle$ of two or four particles. The transition amplitude to states of two particles has contributions from the ϕ^4 and ϕ^2 terms in $\frac{dH}{ds}$. The contribution from the ϕ^2 term is

$$\begin{aligned}
\langle \mathbf{p}_1, \mathbf{p}_2| \sum_{\mathbf{x}\in\Omega} a^d \frac{\delta_m}{2}\phi^2(\mathbf{x})|\mathrm{vac}(0)\rangle &= \sum_{\mathbf{x}\in\Omega} a^d \frac{\delta_m}{L^{2d}} e^{-i(\mathbf{p}_1+\mathbf{p}_2)\cdot\mathbf{x}} \frac{1}{2\sqrt{\omega(\mathbf{p}_1)\omega(\mathbf{p}_2)}} \langle \mathbf{p}_1, \mathbf{p}_2| a^\dagger_{\mathbf{p}_1} a^\dagger_{\mathbf{p}_2}|\mathrm{vac}(0)\rangle \\
&= \sum_{\mathbf{x}\in\Omega} \frac{a^d}{L^d} e^{-i(\mathbf{p}_1+\mathbf{p}_2)\cdot\mathbf{x}} \frac{\delta_m}{2\sqrt{\omega(\mathbf{p}_1)\omega(\mathbf{p}_2)}} \\
&= \frac{\delta_m}{2\omega(\mathbf{p}_1)} \delta_{\mathbf{p}_1+\mathbf{p}_2,0} \\
&= (-\lambda_0\mu^{(1)} - \lambda_0^2\mu^{(2)}) \frac{\delta_{\mathbf{p}_1+\mathbf{p}_2,0}}{2\omega(\mathbf{p}_1)}.
\end{aligned} \tag{S76}$$

The contribution from the ϕ^4 term is

$$\langle \mathbf{p}_1, \mathbf{p}_2| \sum_{\mathbf{x}\in\Omega} a^d \frac{\lambda_0}{4!}\phi^4(\mathbf{x})|\mathrm{vac}(0)\rangle = \lambda_0\mu^{(1)} \frac{\delta_{\mathbf{p}_1+\mathbf{p}_2,0}}{2\omega(\mathbf{p}_1)}, \tag{S77}$$

by the definition of $\mu^{(1)}$ (that is, $\mu^{(1)}$ is the first-order mass correction given by diagram S11).

Thus, the total matrix element for creating two particles is

$$\langle \mathbf{p}_1, \mathbf{p}_2| \frac{dH}{ds}|\mathrm{vac}(0)\rangle = -\lambda_0^2\mu^{(2)} \frac{\delta_{\mathbf{p}_1+\mathbf{p}_2,0}}{2\omega(\mathbf{p}_1)} + O(\lambda_0^3). \tag{S78}$$

Note that this requires tuning of δ_m. The total probability $P^{(2)}_{\mathrm{create}}$ of creating two particles is obtained by summing the squared amplitudes for all possible two-particle outgoing states. Thus, by Eq. S78 and Eq. S74,

$$P^{(2)}_{\mathrm{create}} \sim \frac{J^2\lambda_0^4}{\tau^2}(\mu^{(2)})^2 \sum_{\mathbf{p}\in\Gamma} \frac{1}{\omega(\mathbf{p})^6} \tag{S79}$$

$$\sim \frac{J^2\lambda_0^4 V}{\tau^2}(\mu^{(2)})^2 \int_\Gamma d^d p \frac{1}{(\mathbf{p}^2+m^2)^3}. \tag{S80}$$

(Four powers of $1/\omega(\mathbf{p})$ come from the square of $1/(E_k - E_l)^2$ and two powers come from the square of $\langle \mathbf{p}_1, \mathbf{p}_2 | \frac{dH}{ds} | \mathrm{vac}(0) \rangle$.) For $d = 1, 2, 3$, this integral is non-divergent as $a \to 0$. Thus,

$$P^{(2)}_{\mathrm{create}} = \tilde{O}\left(\frac{J^2 \lambda_0^4 (\mu^{(2)})^2 V}{\tau^2 m^{6-d}} \right) . \tag{S81}$$

By Eq. S69,

$$J = \begin{cases} \tilde{O}\left(\sqrt{\tau}\right) , & d = 1, 2 , \\ \tilde{O}\left(\frac{\sqrt{\tau}}{a}\right) , & d = 3 . \end{cases} \tag{S82}$$

By Eq. S63,

$$\mu^{(2)} = \begin{cases} \tilde{O}(1) , & d = 1, 2 , \\ \tilde{O}(1/a^2) , & d = 3 . \end{cases} \tag{S83}$$

Thus, by Eq. S81, Eq. S82, and Eq. S83,

$$P^{(2)}_{\mathrm{create}} = \begin{cases} \tilde{O}\left(\frac{V}{\tau}\right) , & d = 1, 2 , \\ \tilde{O}\left(\frac{V}{\tau a^6}\right) , & d = 3 . \end{cases} \tag{S84}$$

Next, we consider the amplitude to create four particles. At $s = 0$, the corresponding term in the numerator of Eq. S74 is:

$$\langle \mathbf{p}_1, \mathbf{p}_2, \mathbf{p}_3, \mathbf{p}_4 | \frac{\lambda_0}{4!} \sum_{\mathbf{x} \in \Omega} a^d \phi^4(\mathbf{x}) | \mathrm{vac}(0) \rangle = \frac{\lambda_0 \delta_{\mathbf{p}_1 + \mathbf{p}_2 + \mathbf{p}_3 + \mathbf{p}_4, 0}}{4V \sqrt{\omega(\mathbf{p}_1)\omega(\mathbf{p}_2)\omega(\mathbf{p}_3)\omega(\mathbf{p}_4)}} . \tag{S85}$$

We obtain the probability of excitation due to creation of four particles from the vacuum by substituting the matrix element above into Eq. S74, squaring the resulting amplitude, and summing over all allowed combinations of the four outgoing momenta. Thus,

$$P^{(4)}_{\mathrm{create}} \sim \sum_{\mathbf{p}_1, \mathbf{p}_2, \mathbf{p}_3, \mathbf{p}_4 \in \Gamma} \frac{J^2 \lambda_0^2 \delta_{\mathbf{p}_1 + \mathbf{p}_2 + \mathbf{p}_3 + \mathbf{p}_4, 0}}{V^2 \tau^2 (\omega(\mathbf{p}_1) + \omega(\mathbf{p}_2) + \omega(\mathbf{p}_3) + \omega(\mathbf{p}_4))^4 \omega(\mathbf{p}_1)\omega(\mathbf{p}_2)\omega(\mathbf{p}_3)\omega(\mathbf{p}_4)} . \tag{S86}$$

One can verify that this sum has the following scaling as $a \to 0$:

$$P^{(4)}_{\mathrm{create}} = \begin{cases} \tilde{O}\left(\frac{VJ^2}{\tau^2}\right) , & d = 1, 2 , \\ \tilde{O}\left(\frac{VJ^2}{\tau^2 a}\right) , & d = 3 . \end{cases} \tag{S87}$$

By Eq. S69 and Eq. S87,

$$P^{(4)}_{\text{create}} = \begin{cases} \tilde{O}\left(\frac{V}{\tau}\right), & d = 1, 2, \\ \tilde{O}\left(\frac{V}{\tau a^3}\right), & d = 3. \end{cases} \tag{S88}$$

Finally, we consider the process in which the time dependence of the ϕ^4 term causes a single particle to split into three. For this process, the relevant matrix element is

$$\langle \mathbf{p}_2, \mathbf{p}_3, \mathbf{p}_4 | \frac{\lambda_0}{4!} \sum_{\mathbf{x} \in \Omega} a^d \phi^4(\mathbf{x}) | \mathbf{p}_1 \rangle = \frac{\lambda_0 \delta_{\mathbf{p}_2+\mathbf{p}_3+\mathbf{p}_4, \mathbf{p}_1}}{4V\sqrt{\omega(\mathbf{p}_1)\omega(\mathbf{p}_2)\omega(\mathbf{p}_3)\omega(\mathbf{p}_4)}}, \tag{S89}$$

where $\mathbf{p}_1$ is the momentum of the incoming particle. By our choice of path, the physical mass is s-independent to first order in the coupling, and the s dependence of the coupling is only logarithmically divergent as $a \to 0$. Thus, by Eq. S73,

$$P_{\text{split}} \sim \frac{J^2}{\tau^2 V^2} \sum_{\mathbf{p}_2, \mathbf{p}_3, \mathbf{p}_4 \in \Gamma} \frac{\lambda_0^2 \delta_{\mathbf{p}_2+\mathbf{p}_3+\mathbf{p}_4, \mathbf{p}_1}}{(\omega(\mathbf{p}_2) + \omega(\mathbf{p}_3) + \omega(\mathbf{p}_4) - \omega(\mathbf{p}_1))^4 \omega(\mathbf{p}_1)\omega(\mathbf{p}_2)\omega(\mathbf{p}_3)\omega(\mathbf{p}_4)}. \tag{S90}$$

Let us now examine the divergence structure of P_{split} as $a \to 0$. In the limit of large volume, the sum converges to the following integral:

$$\frac{2J^2}{\tau^2} \int_\Gamma d^d p_2 \int_\Gamma d^d p_3 \frac{\lambda_0^2}{(\omega(\mathbf{p}_2) + \omega(\mathbf{p}_3) + \omega(\mathbf{p}_1 - \mathbf{p}_2 - \mathbf{p}_3) - \omega(\mathbf{p}_1))^4 \omega(\mathbf{p}_1)\omega(\mathbf{p}_2)\omega(\mathbf{p}_3)\omega(\mathbf{p}_1 - \mathbf{p}_2 - \mathbf{p}_3)}.$$

If this were divergent as $a \to 0$, then by approximating the integrand with its value at large $|\mathbf{p}_2|$ and $|\mathbf{p}_3|$, we would be able to isolate the divergence:

$$P_{\text{split}} \sim \frac{J^2 \lambda_0^2}{\tau^2 \omega(\mathbf{p}_1)} \int_\Gamma d^d p_2 \int_\Gamma d^d p_3 \frac{1}{(|\mathbf{p}_2| + |\mathbf{p}_3| + |\mathbf{p}_2 + \mathbf{p}_3|)^4 |\mathbf{p}_2||\mathbf{p}_3||\mathbf{p}_2 + \mathbf{p}_3|}. \tag{S91}$$

However, for $d = 1, 2, 3$, this is convergent as $a \to 0$. Thus, recalling Eq. S69, we obtain

$$P_{\text{split}} = O\left(\frac{J^2}{\tau^2}\right) = \begin{cases} \tilde{O}\left(\frac{1}{\tau}\right), & d = 1, 2, \\ \tilde{O}\left(\frac{1}{\tau a^2}\right), & d = 3. \end{cases} \tag{S92}$$

We can consider two criteria regarding diabatic particle creation. If our detectors are localized, we may be able to tolerate a low constant density of stray particles created during state preparation. This background is similar to that encountered in experiments and may not invalidate conclusions from the simulation. Alternatively, one could adopt a strict criterion by

demanding that, with high probability, not even one stray particle is created in the volume being simulated during state preparation. This strict criterion can be quantified by demanding that the adiabatically produced state has an inner product of at least $1 - \epsilon_{\text{ad}}$ with the exact state. This parameter ϵ_{ad} is thus directly comparable with ϵ_{trunc}, and the two sources of error can be added. Applying the strict criterion, we demand that $P^{(2)}_{\text{split}}$, $P^{(4)}_{\text{split}}$, and P_{create} each be of order ϵ_{ad} and obtain

$$\tau_{\text{strict}} = \begin{cases} \tilde{O}\left(\frac{V}{\epsilon_{\text{ad}}}\right), & d = 1, 2, \\ \tilde{O}\left(\frac{V}{a^6 \epsilon_{\text{ad}}}\right), & d = 3. \end{cases} \tag{S93}$$

Applying the more lenient criterion that $(P^{(2)}_{\text{create}} + P^{(4)}_{\text{create}})/V$ and P_{split} each be of order ϵ_{ad} yields

$$\tau_{\text{lenient}} = \begin{cases} \tilde{O}\left(\frac{1}{\epsilon_{\text{ad}}}\right), & d = 1, 2, \\ \tilde{O}\left(\frac{1}{a^6 \epsilon_{\text{ad}}}\right), & d = 3. \end{cases} \tag{S94}$$

If a k^{th}-order Suzuki-Trotter formula is used, the asymptotic scaling of the total number of gates needed for adiabatic state preparation is $O\left((\mathcal{V}\tau)^{1+\frac{1}{2k}}\right) = O\left((V\tau/a^d)^{1+\frac{1}{2k}})\right)$. Thus,

$$G^{\text{strict}}_{\text{adiabatic}} = \begin{cases} \tilde{O}\left(\left(\frac{V^2}{a^d \epsilon_{\text{ad}}}\right)^{1+\frac{1}{2k}}\right), & d = 1, 2, \\ \tilde{O}\left(\left(\frac{V^2}{a^9 \epsilon_{\text{ad}}}\right)^{1+\frac{1}{2k}}\right), & d = 3. \end{cases} \tag{S95}$$

$$G^{\text{lenient}}_{\text{adiabatic}} = \begin{cases} \tilde{O}\left(\left(\frac{V}{a^d \epsilon_{\text{ad}}}\right)^{1+\frac{1}{2k}}\right), & d = 1, 2, \\ \tilde{O}\left(\left(\frac{V}{a^9 \epsilon_{\text{ad}}}\right)^{1+\frac{1}{2k}}\right), & d = 3. \end{cases} \tag{S96}$$

S.4.2 Strong Coupling

In two and three spacetime dimensions, we can obtain a strongly coupled (that is, non-perturbative) field theory by approaching the phase transition (§ S.3). As in the case of weak coupling, the necessary time for adiabatic state preparation depends on various physical parameters of the system being simulated, including the momentum of the incoming particles, the volume, the strength of the final coupling, the number of spatial dimensions, and the physical mass. To

keep the discussion concise, we restrict our discussion to the case of ultrarelativistic incoming particles, with coupling strength close to the critical value. Under these conditions, the incoming particles can produce a shower of many ($n_{\rm out} \sim p/m$) outgoing particles. Because of the strong coupling, perturbation theory is inapplicable and, even if it could be used, would take exponential computation in the number of outgoing particles.

In the strongly coupled case, we vary the Hamiltonian S5 with s by keeping the bare mass constant at m_0 and setting the bare coupling to $s\lambda_0$. We choose λ_0 only slightly below the critical value λ_c, so that at $s = 1$ the system closely approaches the phase transition, as illustrated in Fig. S1. Examining Eq. S55 suggests that we can estimate phase errors by understanding the behavior of $m^2(s)$ at $s = 0$ and $s = 1$, without needing to know exactly what happens in between. From Eq. S62,

$$\left.\frac{dm^2}{ds}\right|_{s=0} = \begin{cases} \frac{\lambda_0}{8\pi}\log\left(\frac{64}{m_0^2 a^2}\right), & d=1\,, \\ \frac{25.379}{16\pi^2}\frac{\lambda_0}{a}, & d=2\,, \end{cases} \tag{S97}$$

and, from Eq. S13 and Eq. S14,

$$\left.\frac{dm^2}{ds}\right|_{s=1} \sim \begin{cases} -2(\lambda_c-\lambda_0)\,, & d=1\,, \\ -1.26(\lambda_c-\lambda_0)^{0.26}\,, & d=2\,. \end{cases} \tag{S98}$$

Thus, Eq. S58 yields

$$J = \tilde{O}\left(\sqrt{\frac{\tau\lambda_0}{a^{d-1}p^2\mathcal{D}}}\right), \quad d=1,2\,, \tag{S99}$$

under the assumption that $(\lambda_c - \lambda_0)$ is very small.

The result S55 rests on two approximations, a Taylor expansion to second order in Eq. S50 and an approximation of a sum by an integral in Eq. S53. The validity conditions for these approximations become most stringent at $s = 1$, where the derivatives of m^2 with respect to s become large. Working out the $O(J^{-4})$ term in Eq. S55 at $s = 1$, one finds that it will be much smaller than the $O(J^{-2})$ term at $s = 1$ provided

$$J \gg \frac{1}{\lambda_c - \lambda_0}\,. \tag{S100}$$

Similarly, higher-order terms in the Taylor expansion are suppressed by additional powers of $\frac{1}{J(\lambda_c-\lambda_0)}$. The criterion S100 also suffices to justify the approximation of the sum by an integral in Eq. S53.

We must next consider adiabaticity to determine τ. In the ultrarelativistic limit, the relevant energy gap γ corresponds to particle splitting and is $\sim \frac{m^2}{p}$. This takes its minimum value at $s = 1$, namely,

$$\gamma_{\min} \sim \begin{cases} \frac{(\lambda_c-\lambda_0)^2}{p}\,, & d=1\,, \\ \frac{(\lambda_c-\lambda_0)^{1.26}}{p}\,, & d=2\,. \end{cases} \tag{S101}$$

Unlike in the perturbative case, we cannot make a detailed quantitative analysis. However, under the condition S100, the energy gap γ changes only slightly in any adiabatic step (described by Eq. 6 and Eq. S6). Thus we apply the traditional adiabatic approximation Eq. S72 and find that each adiabatic step contributes an excitation amplitude of order $\frac{1}{\tau\gamma^2}$. Depending on the relative phases of the excitation amplitudes arising from the J steps, the total excitation amplitude could be as high as $\frac{J}{\tau\gamma^2}$. Indeed, a detailed analysis suggests that this bound is not overly pessimistic. Thus, to keep the error probability at some small constant $\epsilon_{\rm ad}$, we choose

$$\tau \sim \frac{J}{\gamma^2\sqrt{\epsilon_{\rm ad}}}\,. \tag{S102}$$

We now consider asymptotic scaling with p for fixed λ_0. To achieve continuum-like behavior we need $a \ll \frac{1}{p}$. Thus Eq. S99 yields

$$J \sim \tau^{1/2} p^{(d-3)/2}\,, \quad d=1,2\,. \tag{S103}$$

Substituting Eq. S100 and Eq. S101 into Eq. S102, we see that we need

$$\tau \gtrsim p^2\,, \quad d=1,2\,. \tag{S104}$$

Substituting Eq. S103 and Eq. S101 into Eq. S102, we see that we also need

$$\tau \gtrsim p^{d+1}\,, \quad d=1,2\,. \tag{S105}$$

The scaling $\tau = O(p^{d+1})$ for $d = 1, 2$ suffices to satisfy both conditions S104 and S105. Thus, by the results of §S.5, the total number of gates scales as

$$G_{\text{strong}} = O((V\tau)^{1+o(1)} p^{d+1+o(1)}) \tag{S106}$$

$$= O\left(V^{1+o(1)} p^{2d+2+o(1)}\right), \tag{S107}$$

for $d = 1, 2$.

Next, we consider asymptotic scaling with $(\lambda_c - \lambda_0)$ for fixed p. The J scaling as $\sqrt{\tau}$ in Eq. S99 automatically satisfies the condition S100. Thus, we substitute Eq. S99 into Eq. S102, obtaining

$$\tau \sim \begin{cases} \left(\frac{1}{\lambda_c - \lambda_0}\right)^8, & d = 1, \\ \left(\frac{1}{\lambda_c - \lambda_0}\right)^{5.04}, & d = 2. \end{cases} \tag{S108}$$

The spacing between particles in the in and out states must be of order $1/m$. Thus, with constant a, $\mathcal{V} \sim 1/(\lambda_c - \lambda_0)^{\nu d}$. If a k^{th}-order Suzuki-Trotter formula is used, the necessary number of quantum gates G_{strong} scales as $O\left((\mathcal{V}\tau)^{1+\frac{1}{2k}}\right)$. Thus,

$$G_{\text{strong}} \sim \begin{cases} \left(\frac{1}{\lambda_c - \lambda_0}\right)^{9\left(1+\frac{1}{2k}\right)}, & d = 1, \\ \left(\frac{1}{\lambda_c - \lambda_0}\right)^{6.3\left(1+\frac{1}{2k}\right)}, & d = 2. \end{cases} \tag{S109}$$

Note that one could improve this scaling by choosing a more optimized adiabatic state-preparation schedule, which slows down as the gap gets smaller.

S.5 Suzuki-Trotter Formulae for Large Lattices

It appears that, while scaling with t has been thoroughly studied, little attention has been given to scaling of quantum simulation algorithms with the number of lattice sites, $\mathcal{V}$. Using a result of Suzuki and elementary Lie algebra theory, we derive linear scaling provided the Hamiltonian is local.

For any even k and any pair of Hamiltonians A, B,

$$\left(e^{iA\alpha_1 t/n}e^{iB\beta_1 t/n}e^{iA\alpha_2 t/n}e^{i\beta_2 Bt/n}\dots e^{iA\alpha_r t/n}\right)^n = e^{i(A+B)t} + O(t^{2k+1}/n^{2k})\,, \tag{S110}$$

where $r = 1 + 5^{k/2-1}$ and $\alpha_1, \dots, \alpha_r, \beta_1, \dots, \beta_{r-1}$ are specially chosen coefficients such that $\sum_{j=1}^{r} \alpha_j = 1$ and $\sum_{j=1}^{r-1} \beta_j = 1$ (*34*). Thus, using the k^{th}-order Suzuki-Trotter formula (Eq. S110), one can simulate evolution for time t with $O\left(t^{\frac{2k+1}{2k}}\right)$ quantum gates (*35*). To determine the $\mathcal{V}$ scaling, we use the following standard theorem (cf. the Baker-Campbell-Hausdorff formula).

Theorem 1 *Let A and B be elements of a Lie algebra defined over any field of characteristic 0. Then $e^A e^B = e^C$, where C is a formal infinite sum of elements of the Lie algebra generated by A and B.*

A and B generate a Lie algebra by commutation and linear combination. Thus, without requiring any explicit calculation, Theorem 1 together with Eq. S110 implies

$$\left(e^{iA\delta_1 t/n}e^{iB\delta_2 t/n}\dots e^{iA\delta_r t/n}\right)^n = e^{i(A+B)t} + \Delta_{2k+1}t^{2k+1}/n^{2k} + O(n^{-(2k+1)})\,, \tag{S111}$$

where Δ_{2k+1} is a linear combination of nested commutators. In general, $\|\Delta_{2k+1}\|$ could be as large as $(\max\{\|A\|, \|B\|\})^{2k+1}$. However, by the canonical commutation relations, one sees that, for the pair of local Hamiltonians H_ϕ, H_π, $\|\Delta_{2k+1}\| = O(\mathcal{V})$, for any fixed k. Thus, one needs only $n = O\left(t^{\frac{2k+1}{2k}}\mathcal{V}^{\frac{1}{2k}}\right)$. Recalling the $O(\mathcal{V})$ cost for simulating each $e^{iH_\phi \delta t}$ or $e^{iH_\pi \delta t}$, one sees that the total number of gates scales as $O\left((t\mathcal{V})^{1+\frac{1}{2k}}\right)$. Note that this conclusion may be of general interest, as it applies to any lattice Hamiltonian for which non-neighboring terms commute.

In the case of strong coupling, we care not only about how the number of gates scales with $\mathcal{V}$ but also about scaling with p. In the presence of high-energy incoming particles, the field can have large distortions from its vacuum state. For example, if $\langle\psi|\phi(\mathbf{x})|\psi\rangle$ is large, then local

terms in $\Delta_{2k+1}|\psi\rangle$ such as $\pi(\mathbf{x})\phi(\mathbf{x})^3|\psi\rangle$ can become large. We can obtain a heuristic upper bound on this effect by noting that, in the strongly coupled case, $m_0^2 > 0$, so each local term in H is a positive operator. Thus, if $\langle\psi|H|\psi\rangle \leq E$, then the expectation value of each of the local terms is bounded above by E. Using E as a simple estimate of the maximum magnitude of a local term, we see that $\Delta_{2k+1}|\psi\rangle$, which is a sum of $O(\mathcal{V})$ terms, each of which is of degree $2k+1$ in the local terms of H, has magnitude at most $O(\mathcal{V}E^{2k+1})$, or in other words $O(\mathcal{V}p^{2k+1})$. Recalling that a scales as a small multiple of $1/p$, we see that $\Delta_{2k+1}|\psi\rangle = O(Vp^{2k+1+d})$. Thus, $n = O(p^{1+(1+d)/2k}t^{1+1/2k})$. Each timestep requires $O(\mathcal{V}) = O(Vp^d)$ gates to implement. Thus, the overall scaling is $O(p^{d+1+o(1)}(tV)^{1+o(1)})$ quantum gates to simulate the strongly coupled theory at large p.

S.6 Simulating Detectors

In some scattering processes, especially at strong coupling, the outgoing particles may be in bound states. In this case, it may not be desirable to adiabatically turn off the coupling and measure the occupation numbers of momentum modes of the free theory. Instead, we can divide space into regions and measure the total energy and momentum within each region. If the regions are small compared with the separation between particles (some of which may be composite), then each region contains at most one particle, and we obtain its energy and spatial momentum. There is some probability that multiple particles are in a single region, in which case our simulated "detector" fails to resolve them. This is reasonably analogous to real detectors, which have finite resolution and do not involve adiabatic turn-off of the coupling.

To measure the energy in a region $R \subseteq \Omega$, we simply truncate the Hamiltonian, restricting it to R:

$$H[R] = \sum_{\mathbf{x}\in R} a^d \left[\frac{1}{2}\pi(\mathbf{x}) + \frac{1}{2}\left(\nabla_a\phi\right)^2(\mathbf{x}) + \frac{1}{2}m_0^2\phi(\mathbf{x})^2 + \frac{\lambda_0}{4!}\phi(\mathbf{x})^4\right]. \tag{S112}$$

By the canonical commutation relations, $[H[R], H[R']] = 0$ whenever R and R' are disjoint. (One must decide how to treat discretized derivatives $(\nabla_a \phi)$ that span the boundary of R. We define $H[R]$ to omit these terms. This leaves "cracks" of size a between detectors, which should be negligible for small a.) We can thus tile our simulated volume and measure $H[R]$ for each of the $O\left(\frac{\mathcal{V}}{|R|}\right)$ regions. One can use phase estimation to measure energy to precision Δ_E in a region R by implementing $e^{-iH[R]t}$ for $t \sim \frac{1}{\Delta_E}$. $e^{-iH[R]/\Delta_E}$ can be implemented with $O\left((|R|/\Delta_E)^{1+o(1)}\right)$ quantum gates (§ S.5). Thus, the total number G_{energy} of quantum gates needed to measure the energy in every region scales as

$$G_{\text{energy}} = O\left(\mathcal{V}|R|^{o(1)}\Delta_E^{-1-o(1)}\right). \tag{S113}$$

Note that G_{energy} scales as p^{d+1} rather than p^d, as one might naively expect (see Sec. S.5). Note also that the energy of the vacuum is non-zero, and we must subtract this to obtain particle energies.

Next, we consider how to measure momentum. Noether's theorem dictates that the momentum operators for a continuum scalar theory (either interacting or non-interacting) are

$$P_j = -\int d^d x \pi(\mathbf{x}) \frac{d}{dx_j} \phi(\mathbf{x}), \tag{S114}$$

for $j = 1, \ldots, d$. To obtain Hermitian discretization of these operators, we define

$$P_j^{(a)} = -\sum_{\mathbf{x}\in\Omega} a^d \left[\pi(\mathbf{x}) \left(\frac{\phi(\mathbf{x} + a\hat{r}_j) - \phi(\mathbf{x} - a\hat{r}_j)}{2a}\right)\right]. \tag{S115}$$

If we assume $a \ll \frac{1}{p}$, then $P_j^{(a)}$ provides a good approximation to the continuum operator P_j.

Let

$$P_j^{(a)}(\mathbf{x}) = -a^d \pi(\mathbf{x}) \left(\frac{\phi(\mathbf{x} + a\hat{r}_j) - \phi(\mathbf{x} - a\hat{r}_j)}{2a}\right) \tag{S116}$$

and

$$P_j^{(a)}[R] = \sum_{\mathbf{x}\in R} P_j^{(a)}(\mathbf{x}). \tag{S117}$$

$P_j[R]$ can be interpreted as measuring the total momentum along the j axis in the region R. One can see that

$$\left[P_j^{(a)}(\mathbf{x} + 2a\hat{r}_j), P_j^{(a)}(\mathbf{x})\right] = 0\,. \tag{S118}$$

Thus, we can decompose $P_j^{(a)}[R]$ into two operators, each of which is a sum of commuting local terms, as follows:

$$\begin{aligned} P_j^{(a)}[R] &= P_j^{(a)}[R_j^{\text{even}}] + P_j^{(a)}[R_j^{\text{odd}}]\,, & \text{(S119)} \\ R_j^{\text{even}} &= \{(x_1, \ldots, x_d) \in R | x_j/a \text{ even}\}\,, & \text{(S120)} \\ R_j^{\text{odd}} &= \{(x_1, \ldots, x_d) \in R | x_j/a \text{ odd}\}\,. & \text{(S121)} \end{aligned}$$

By Eq. S118, the time evolutions induced by $P_j^{(a)}[R_j^{\text{even}}]$ and $P_j^{(a)}[R_j^{\text{odd}}]$ are both easy to simulate, because

$$\exp\left[-iP_j^{(a)}[R_j^{\text{odd}}]t\right] = \prod_{\mathbf{x}\in R_j^{\text{odd}}} \exp\left[-iP_j^{(a)}(\mathbf{x})t\right], \tag{S122}$$

with an analogous equation for the even case. To measure the observable $P_j^{(a)}[R]$ via phase estimation, we must simulate time evolution induced by the sum of $P_j^{(a)}[R_j^{\text{even}}]$ and $P_j^{(a)}[R_j^{\text{odd}}]$. To do so, one can use high-order Trotter formulae. By the analysis of Sec. S.5, the total complexity G_P of measuring momentum in every region scales as

$$G_P = O\left(\left(|R|^{o(1)}\frac{\mathcal{V}}{\Delta_P}\right)^{1+o(1)}\right). \tag{S123}$$

Note that Δ_P is also limited, via the uncertainty principle, by the size of R.

S.7 Minimal Qubit Requirement

In this section, we estimate the number of qubits needed for a minimal non-trivial demonstration of our algorithm. Specifically, to simulate a $2 \to 4$ scattering process in $1+1$ dimensions, on the order of a thousand to ten thousand qubits should suffice, depending on the desired level of

precision (see Fig. S2). Note that we assume the qubits and quantum gates are noiseless. A large number of noisy physical qubits can substitute for a smaller number of perfect "logical" qubits through the use of quantum error correction (see, for example, (*47*)). The ratio of physical to logical qubits depends not only on the quantum error-correction scheme but also on the particular implementation chosen (for example, trapped ions versus superconducting qubits) and the experimental techniques for reducing sources of noise, which are beyond the scope of this paper.

We must choose E to be at least $4m$ so that $2 \to 4$ scattering is kinematically allowed. (Actually, one should choose E slightly larger than $4m$ so that the process is not suppressed by the lack of phase space to scatter into.) Thus, we choose $E = 5m$, which implies

$$p/m \simeq 2. \tag{S124}$$

By our EFT analysis, discretization errors in scattering events with momentum p are of order $(pa)^2$. Setting this to ϵ and using Eq. S124, we obtain

$$ma \simeq \frac{\sqrt{\epsilon}}{2}\,. \tag{S125}$$

To estimate the total number of qubits, we must determine what are sufficient numbers of lattice sites and qubits per site. Without a sufficient number of lattice sites, the incoming and outgoing particles cannot be well separated. Thus, the interparticle force will be non-negligible, and the in and out states created will not be a good approximation to the asymptotic in and out states that define the S-matrix.

Calculating to second order in λ and applying the (non-relativistic) Born approximation (a good approximation for λ sufficiently small), one finds that, for $D = 2$, the interparticle potential at large r is

$$V^{(2)}(r \to \infty) = -\frac{\lambda^2}{32m^3}\frac{1}{\sqrt{\pi m r}}e^{-2mr}\,. \tag{S126}$$

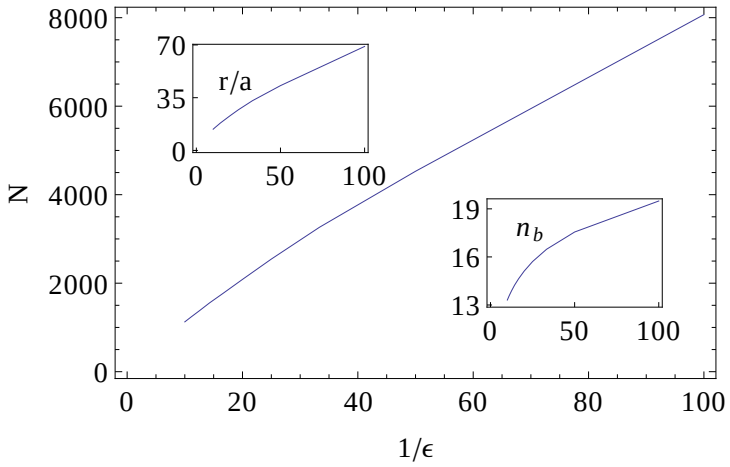

Figure S2: The required number of qubits is shown for $2 \to 4$ scattering as a function of $1/\epsilon$. The insets display the interparticle separation in lattice units (r/a) and the number of qubits per site (n_b), each as a function of $1/\epsilon$. Our estimate N for the total number of qubits is $6 \times (r/a) \times n_b$. The prefactor six is chosen (somewhat arbitrarily) to provide enough space for four outgoing particles to be well separated, with an extra factor of 1.5 to allow for the possibility that they are not evenly spaced.

We want substantial scattering to occur when the particles most closely approach one another, but scattering not to occur when the particles are separated in their in and out states. The expectation value of the distance of closest approach is on the order of the wavepacket width. The wavepacket width should not be chosen much larger than the range of the interaction ($\sim 1/m$), or scattering will be unlikely. We thus demand that $F(r) \ll F(1/m)$, where F is the (magnitude of) the interparticle force. Quantitatively, we can demand

$$\frac{F(r)}{F(1/m)} \leq \epsilon \,. \tag{S127}$$

By numerically solving Eq. S127 and using Eq. S124, one obtains the inset shown in Fig. S2.

Next, we estimate the necessary number of qubits per site. In Sec. S.4, the constant factors hidden by the big-O notation can easily be restored. Specifically, a sufficient choice is

$$n_b = \left\lceil \log_2 \left(1 + \frac{2a^d}{\pi} \left(1 + \sqrt{\frac{\mathcal{V}}{\epsilon}} \right)^2 \sqrt{\langle \phi^2 \rangle \langle \pi^2 \rangle} \right) \right\rceil . \tag{S128}$$

To bound $\langle\phi^2\rangle$ and $\langle\pi^2\rangle$, we must estimate the bare quantities λ_0 and m_0^2 and then apply Proposition 3 or 4. In $D = 2$, one finds perturbatively that

$$m_0^2 = m^2 - \frac{\lambda}{8\pi}\log\left(\frac{64}{m^2a^2}\right) + \cdots , \tag{S129}$$

$$\lambda_0 = \lambda + \frac{3\lambda^2}{8\pi m^2} + \cdots . \tag{S130}$$

We must now choose a value of λ that is small enough to justify the use of $V^{(2)}$, but large enough to make classical calculations at high precision difficult. As concrete examples, we consider the values $\frac{\lambda}{2\pi m^2} = \frac{1}{3}$ and $\frac{\lambda}{2\pi m^2} = \frac{1}{10}$. The results show that n_b is not very sensitive to the choice of λ, as discussed below.

For $0.01 \leq \epsilon \leq 0.1$, our choices of λ and ma imply that $m_0^2 \geq 0$, and thus the applicable bound on $\langle\phi^2\rangle$ and $\langle\pi^2\rangle$ is Proposition 3 throughout the entire adiabatic state preparation. By Eq. S128 and Proposition 3, one obtains n_b as a function of ϵ, as shown in the inset to Fig. S2. Replacing $\frac{\lambda}{2\pi m^2} = \frac{1}{3}$ with $\frac{\lambda}{2\pi m^2} = \frac{1}{10}$ changes n_b from 20 to 19 at $\epsilon = 0.01$ and leaves n_b unchanged at 13 for $\epsilon = 0.1$.

Finally, let us comment on the asymptotic scaling of the number of qubits required by our algorithm. As discussed above (see Eq. S125), to restrict discretization errors to order ϵ we need $ma \sim \sqrt{\epsilon}$. Furthermore, to obtain good in and out states we need particles to be separated by a distance $r \sim \frac{1}{m}\log(1/\epsilon)$. Thus, the total number of lattice sites is $\mathcal{V} \sim \left(\frac{r}{a}\right)^d = O\left(\epsilon^{-d/2}\log^d(1/\epsilon)\right)$. The number of qubits per site is $n_b \sim \log(1/\epsilon)$. Thus, the total number of qubits is $N = O\left(\epsilon^{-d/2}\log^{d+1}(1/\epsilon)\right)$. In contrast to the estimate shown in Fig. S2, which relies on perturbative calculations, this asymptotic scaling should hold at both strong and weak coupling. Note that, as mentioned in § S.1, we consider spatially localized wavepackets and the attendant uncertainty in momentum to be physically realistic and not a source of error, although this notion differs from the idealization used to define an S-matrix.

References

1. R. P. Feynman, Simulating physics with computers. *Int. J. Theor. Phys.* **21**, 467 (1982). doi:10.1007/BF02650179

2. S. Lloyd, Universal quantum simulators. *Science* **273**, 1073 (1996). doi:10.1126/science.273.5278.1073 Medline

3. D. S. Abrams, S. Lloyd, Simulation of many-body Fermi systems on a universal quantum computer. *Phys. Rev. Lett.* **79**, 2586 (1997). doi:10.1103/PhysRevLett.79.2586

4. C. Zalka, Simulating quantum systems on a quantum computer. *Proc. R. Soc. London Ser. A* **454**, 313 (1998). doi:10.1098/rspa.1998.0162

5. B. P. Lanyon *et al*., Universal digital quantum simulation with trapped ions. *Science* **334**, 57 (2011). doi:10.1126/science.1208001 Medline

6. M. Müller, K. Hammerer, Y. L. Zhou, C. F. Roos, P. Zoller, Simulating open quantum systems: From many-body interactions to stabilizer pumping. *New J. Phys.* **13**, 085007 (2011). doi:10.1088/1367-2630/13/8/085007

7. J. T. Barreiro *et al*., An open-system quantum simulator with trapped ions. *Nature* **470**, 486 (2011). doi:10.1038/nature09801 Medline

8. J. Glimm, A. Jaffe, ϕ_2^4 quantum field model in the single-phase region: Differentiability of the mass and bounds on critical exponents. *Phys. Rev. D* **10**, 536 (1974). doi:10.1103/PhysRevD.10.536

9. F. Guerra, L. Rosen, B. Simon, Correlation inequalities and the mass gap in $P(\phi)_2$ III. Mass gap for a class of strongly coupled theories with nonzero external field. *Commun. Math. Phys.* **41**, 19 (1975). doi:10.1007/BF01608544

10. O. A. McBryan, J. Rosen, Existence of the critical point in ϕ^4 field theory. *Commun. Math. Phys.* **51**, 97 (1976). doi:10.1007/BF01609341

11. K. Osterwalder, R. Sénéor, The scattering matrix is nontrivial for weakly coupled $P(\phi)_2$ models. *Helv. Phys. Acta* **49**, 525 (1976).

12. J.-P. Eckmann, H. Epstein, J. Fröhlich, Asymptotic perturbation expansion for the S-matrix and the definition of time ordered functions in relativistic quantum field models. *Ann. Inst. Henri Poincaré A* **25**, 1 (1976).

13. F. Constantinescu, Nontriviality of the scattering matrix for weakly coupled ϕ_3^4 models. *Ann. Phys.* **108**, 37 (1977). doi:10.1016/0003-4916(77)90349-9

14. T. Byrnes, Y. Yamamoto, Simulating lattice gauge theories on a quantum computer. *Phys. Rev. A* **73**, 022328 (2006). doi:10.1103/PhysRevA.73.022328

15. H. P. Büchler, M. Hermele, S. D. Huber, M. P. A. Fisher, P. Zoller, Atomic quantum simulator for lattice gauge theories and ring exchange models. *Phys. Rev. Lett.* **95**, 040402 (2005). doi:10.1103/PhysRevLett.95.040402 Medline

16. E. Zohar, B. Reznik, Confinement and lattice quantum-electrodynamic electric flux tubes simulated with ultracold atoms. *Phys. Rev. Lett.* **107**, 275301 (2011). doi:10.1103/PhysRevLett.107.275301 Medline

17. G. Szirmai, E. Szirmai, A. Zamora, M. Lewenstein, Gauge fields emerging from time reversal symmetry breaking for spin-5/2 fermions in a honeycomb lattice. *Phys. Rev. A* **84**, 011611(R) (2011).

18. J. I. Cirac, P. Maraner, J. K. Pachos, Cold atom simulation of interacting relativistic quantum field theories. *Phys. Rev. Lett.* **105**, 190403 (2010). doi:10.1103/PhysRevLett.105.190403 Medline

19. L. Mazza *et al*., An optical-lattice-based quantum simulator for relativistic field theories and topological insulators. *New J. Phys.* **14**, 015007 (2012). doi:10.1088/1367-2630/14/1/015007

20. E. Kapit, E. Mueller, Optical-lattice Hamiltonians for relativistic quantum electrodynamics. *Phys. Rev. A* **83**, 033625 (2011). doi:10.1103/PhysRevA.83.033625

21. A. Bermudez *et al*., Wilson fermions and axion electrodynamics in optical lattices. *Phys. Rev. Lett.* **105**, 190404 (2010). doi:10.1103/PhysRevLett.105.190404 Medline

22. P. Maraner, J. K. Pachos, Yang-Mills gauge theories from simple fermionic lattice models. *Phys. Lett. A* **373**, 2542 (2009). doi:10.1016/j.physleta.2009.05.029

23. L. Lepori, G. Mussardo, A. Trombettoni, (3+1) massive Dirac fermions with ultracold atoms in frustrated cubic optical lattices. *Europhys. Lett.* **92**, 50003 (2010). doi:10.1209/0295-5075/92/50003

24. K. Maeda, G. Baym, T. Hatsuda, Simulating dense QCD matter with ultracold atomic boson-fermion mixtures. *Phys. Rev. Lett.* **103**, 085301 (2009). doi:10.1103/PhysRevLett.103.085301 Medline

25. Á. Rapp, G. Zaránd, C. Honerkamp, W. Hofstetter, Color superfluidity and "baryon" formation in ultracold fermions. *Phys. Rev. Lett.* **98**, 160405 (2007). doi:10.1103/PhysRevLett.98.160405 Medline

26. H. Weimer, M. Müller, I. Lesanovsky, P. Zoller, H. P. Büchler, A Rydberg quantum simulator. *Nat. Phys.* **6**, 382 (2010). doi:10.1038/nphys1614

27. J. Casanova *et al*., Quantum simulation of quantum field theories in trapped ions. *Phys. Rev. Lett.* **107**, 260501 (2011). doi:10.1103/PhysRevLett.107.260501 Medline

28. J. Casanova, A. Mezzacapo, L. Lamata, E. Solano, http://arxiv.org/abs/1110.3730 (2011).

29. B. Douçot, L. B. Ioffe, J. Vidal, Discrete non-Abelian gauge theories in Josephson-junction arrays and quantum computation. *Phys. Rev. B* **69**, 214501 (2004). doi:10.1103/PhysRevB.69.214501

30. M. Lewenstein *et al*., Ultracold atomic gases in optical lattices: Mimicking condensed matter physics and beyond. *Adv. Phys.* **56**, 243 (2007). doi:10.1080/00018730701223200

31. M. Johanning, A. Varón, C. Wunderlich, Quantum simulations with cold trapped ions. *J. Phys. B* **42**, 154009 (2009). doi:10.1088/0953-4075/42/15/154009

32. For $\lambda_0 > 0$ one has a tighter bound. In this case it is unlikely for $|\phi(\mathbf{x})|$ to be much larger than $O(E^{1/4})$.

33. See supplementary materials on *Science* Online.

34. M. Suzuki, Fractal decomposition of exponential operators with applications to many-body theories and Monte Carlo simulations. *Phys. Lett. A* **146**, 319 (1990). doi:10.1016/0375-9601(90)90962-N

35. D. Berry, G. Ahokas, R. Cleve, B. C. Sanders, Efficient quantum algorithms for simulating sparse Hamiltonians. *Commun. Math. Phys.* **270**, 359 (2007). doi:10.1007/s00220-006-0150-x

36. A. Kitaev, W. A. Webb, http://arxiv.org/abs/0801.0342 (2008).

37. J. R. Bunch, J. E. Hopcroft, Triangular factorization and inversion by fast matrix multiplication. *Math. Comput.* **28**, 231 (1974). doi:10.1090/S0025-5718-1974-0331751-8

38. D. Coppersmith, S. Winograd, Matrix multiplication via arithmetic progressions. *J. Symbolic Comp.* **9**, 251 (1990). doi:10.1016/S0747-7171(08)80013-2

39. M. E. Peskin, D. V. Schroeder, *An Introduction to Quantum Field Theory* (Westview, Boulder, CO, 1995).

40. A. Y. Kitaev, http://arxiv.org/abs/quant-ph/9511026 (1995).

41. C. Arzt, Reduced effective Lagrangians. *Phys. Lett. B* **342**, 189 (1995). doi:10.1016/0370-2693(94)01419-D

42. H. Georgi, On-shell effective field theory. *Nucl. Phys. B* **361**, 339 (1991). doi:10.1016/0550-3213(91)90244-R

43. J. C. Le Guillou, J. Zinn-Justin, Critical exponents for the *n*-vector model in three dimensions from field theory. *Phys. Rev. Lett.* **39**, 95 (1977). doi:10.1103/PhysRevLett.39.95

44. M. Lüscher, P. Weisz, Scaling laws and triviality bounds in the lattice ϕ^4 theory (I). One-component model in the symmetric phase. *Nucl. Phys. B* **290**, 25 (1987).

45. A. Messiah, *Quantum Mechanics* (Dover, 1999). (Reprint of the two-volume edition published by Wiley, 1961–1962.)

46. S. Jansen, M.-B. Ruskai, R. Seiler, Bounds for the adiabatic approximation with applications to quantum computation. *J. Math. Phys.* **48**, 102111 (2007). doi:10.1063/1.2798382

47. D. Gottesman, An introduction to quantum error correction and fault-tolerant quantum computation. *Proc. Sympos. Appl. Math.* **68**, 13 (2010).